UNIVERSITY OF OKLAHOMA

GRADUATE COLLEGE

DESIGNING A SUBSTRATE HEATER FOR THIN-FILM DEPOSITION IN HIGH VACUUM

A THESIS

SUBMITTED TO THE GRADUATE FACULTY

in partial fulfillment of the requirements for the

Degree of

Master of Science in Mechanical Engineering

By

BRYAN BOONE

Norman, Oklahoma

2020

DESIGNING A SUBSTRATE HEATER FOR

THIN-FILM DEPOSITION IN HIGH VACUUM

A THESIS APPROVED FOR THE

SCHOOL OF AEROSPACE AND MECHANICAL ENGINEERING

BY THE COMMITTEE CONSISTING OF

Dr. Yingtao Liu

Dr. Lloyd Bumm

Dr. Hamidreza Shabgard

© Copyright by Bryan Boone 2020

All Rights Reserved.

Contents

1 Introduction **1**

2 Design Outline **4**

2.1 Water-Cooled Walls 9

2.2 Lid 12

2.3 Actuated Heat-Sink 15

2.4 Shutter-Cart 18

2.5 Rails 20

2.6 Actuation 22

3 Mathematical Analysis **23**

3.1 Radiative Heat Transfer Calculations 23

3.2 Water Flow Heat Transfer Calculations 28

4 CFD Analysis and Validation **30**

5 Use, Troubleshooting, and Future Application **37**

5.1 Intended Use Procedure 37

5.2 Troubleshooting 38

5.3 Future Applications 39

6 Conclusion **41**

7 Acknowledgments **42**

8 Drawings **43**

9 Appendices **63**

References **73**

List of Figures

1 An illustration of what a very simple thermal evaporation deposition system might look like. This includes the shutter, which is necessary to manage how much of the deposition reaches the substrate. 4
2 An illustration showing the way mated surfaces can be in imperfect conductive contact while under vacuum. Notably, the substrate is shown as perfectly flat, but this is because the Bumm group's substrate of choice, mica, cleaves to atomically flat surfaces. 6
3 A very simply presented form of the heater and integrated equipment proposed, with labels denoting what each color-coded piece represents. 7
4 A CAD rendering of the components designed and the base they are installed onto. 8
5 The 3D model of the heater's walls, the insulating tantalum sheets, and the brazed VCR fittings which connect to the internal water lines. 9
6 The 3D model of the heater's walls, with transparency enabled such that the water-cooling lines are visible. 11
7 An illustration of the way the lid was intended to be separated from the rest of the equipment, to ease access to the substrate. 12
8 The heater's lid, isolated from the rest of the CAD assembly 13
9 The underside of the heater's lid, isolated from the rest of the CAD assembly . . . 14
10 A simple presentation of how an actuated heat-sink could be manipulated to touch, or not touch, the alumina heater. 15
11 The model for the assembly of the actuated heat-sink. The heat-sink itself can be seen as the copper cylinder at the bottom of the image. 17

12 The shutter-cart, as modeled. At each of the four corners there's a bearing which is fastened such that it can freely rotate, and act as the "wheels" of the shutter-cart. 19

13 The rails and their associated structures, the plate which the heater rests upon and the posts which carry the entire structure, with two posts omitted for visual clarity. . 21

14 A volume rendering of the walls' temperature at a steady-state operating condition defined in the text. 33

15 A rendering of the surface temperature within the cooling lines during operating conditions. 34

16 A rendering showing the simulated water pressure at the outlet while operating, notably approximating the average pressure across the entire outlet rather than delineating areas of high and low pressure. 36

List of Tables

1 A table delimiting the degree of vacuum and corresponding pressure range, and other notable qualities of vacuum (λ is the mean free path, and d denotes major diameter) [11]. 2

2 The anticipated wattage to maintain 1000 ° C for a given number of tantalum layers, and the subsequent reduction in wattage each additional layer facilitates . . 27

Abstract

This thesis outlines the design of a custom substrate heater for use in physical vapor deposition of laboratory thin films. Traditional substrate heaters bring a substrate to temperature through a reliance on the conductive heat transfer of a single side of the substrate. Within a vacuum this mode of heat transfer suffers, due to the imperfectly mated conductive surfaces of the substrate and heater. In contrast, this design sandwiches the substrate between two heaters to provide both the traditional conductive heat as well as radiative heat transfer from the opposing heater. In combination with an intricate insulating structure, which off-the-shelf heaters do not generally provide, this design can efficiently bring substrates to a more uniform temperature, which results in the growth of a higher-quality thin film. It also accommodates an integrated heat-sink to quickly cool the substrate and deposition for handling, despite the insulating materials.

Chapter 1

Introduction

The Bumm research group within the Homer L. Dodge Department of Physics and Astronomy studies condensed matter physics, specifically surface physics at the nanometer scale. Recent advancements in supercomputing and microscopy have made direct measure of nanoscale properties in thin films achievable, and thus a priority for the Bumm research group's work. This work requires atomically flat, crystalline grains of metal thin films to act as substrates in scanning tunneling microscopy studies. Thin films are layers of material in the micrometer to nanometer range of thickness with a wide variety of uses. Thin films are a useful research subject for the study of surface physics, which is used heavily in the further miniaturization of transistors. The breakthrough which led to the invention of the metal-oxide-semiconductor field-effect transistor, or MOSFET, was the controlled growth of thin layers of silicon oxide on silicon wafers using thermal oxidation and the surface physics which governed this reaction. The MOSFET lead directly to the microchip revolution and then the digital revolution [1]. Less than a decade after the MOSFET the first thin-film transistor was created, which was eventually used and made essential in the production of LCD screens which are now a part of daily life [4].

Certain commercial suppliers produce thin films for research use [6, 10], but the ability to produce bespoke films on-site can be more cost effective while also allowing for unique film compositions that suppliers can't provide. Some materials, like silver, would tarnish in the time between commercial manufacture and delivery onsite. This is clearly undesirable if one is wishing to study a film made of silver, rather than silver sulfide. The reason many labs choose to buy films instead of making them onsite is that the required equipment is very costly.

Thermal deposition within a high, or ultra-high, vacuum is very simple way to produce thin films. These levels of vacuum are not universally defined, but are generally accepted as falling within the ranges presented by Table 1. In fact, the process is so simple that even Edison was able to perform various depositions within vacuum, filing patents in 1880 and utilizing gold deposi-

	Rough vacuum	Medium vacuum	High vacuum	Ultrahigh vacuum
Pressure (mbar)	10^3 – 1	1 – 10^{-3}	10^{-3} – 10^{-7}	$<10^{-7}$
Particle density (cm^{-3})	10^{19} – 10^{16}	10^{16} – 10^{13}	10^{13} – 10^{9}	$<10^{9}$
Mean free path λ (cm)	$<10^{-2}$	10^{-2} – 10	10 – 10^5	$>10^5$
Monolayer time (s)	$<10^{-5}$	10^{-5} – 10^{-2}	10^{-2} – 10^2	$>10^2$
Type of gas flow Knudsen number $K=\lambda/d$	Viscous flow $K< 10^{-2}$	Knudsen flow $K\approxeq 1$	Molecular flow $K> 10^2$	

Table 1: A table delimiting the degree of vacuum and corresponding pressure range, and other notable qualities of vacuum (λ is the mean free path, and d denotes major diameter) [11].

tion in a process of strengthening phonograph masters for mass production from 1901 to 1921 [12]. The ubiquity of this process partially contributed to the impetus for this project, as a Varian 3118 vacuum chamber was inherited by the Bumm group and thus provided the base, and most expensive component, of the necessary equipment and accessories. Despite being manufactured decades ago, it was fully compliant with ConFlat® components which are still widely available commercially, offering a starting point to design a substrate heater for thin film manufacture.

While commercial solutions do exist for substrate heating, creating a fully custom setup offers opportunities to prioritize the expected use-case of the heater. Of particular note is the need to efficiently reach high, uniform temperatures. This uniformity is important to the quality of films produced through Volmer-Weber growth, which is the simplest achievable growth mode for the equipment and budget of the Bumm group. Excess heat inside the chamber poses a hazard to not only the deposited film's quality but also the physical integrity of the chamber. Through an intricate arrangement of radiative heat insulating tantalum sheets within a water-cooled copper block, this design can effectively heat substrates to temperatures as high as 1000° C. The utility of the insulation during heating is met and contradicted by an actuated heat-sink once the film is finished and needs to be removed. This heat-sink descends to conduct heat out of the ceramic body which holds the substrate and out to the cooling lines of the equipment's exterior. This quickly brings the equipment back down to a manageable temperature thus increasing the operating effi-

ciency of the setup.

Chapter 2

Design Outline

Thermal evaporation and deposition requires both a source to evaporate and a substrate to adsorb the gaseous particles. This project dealt with the substrate, more specifically an assembly to dramatically improve upon the temperature uniformity of the substrate offered by the traditional heater. Traditional commercial heaters require the purchaser to provide and implement ubiquitous additional components, such as insulation and cooling means. While deposition is possible without these additional components, as seen in Figure 1 below, it can be significantly more complex.

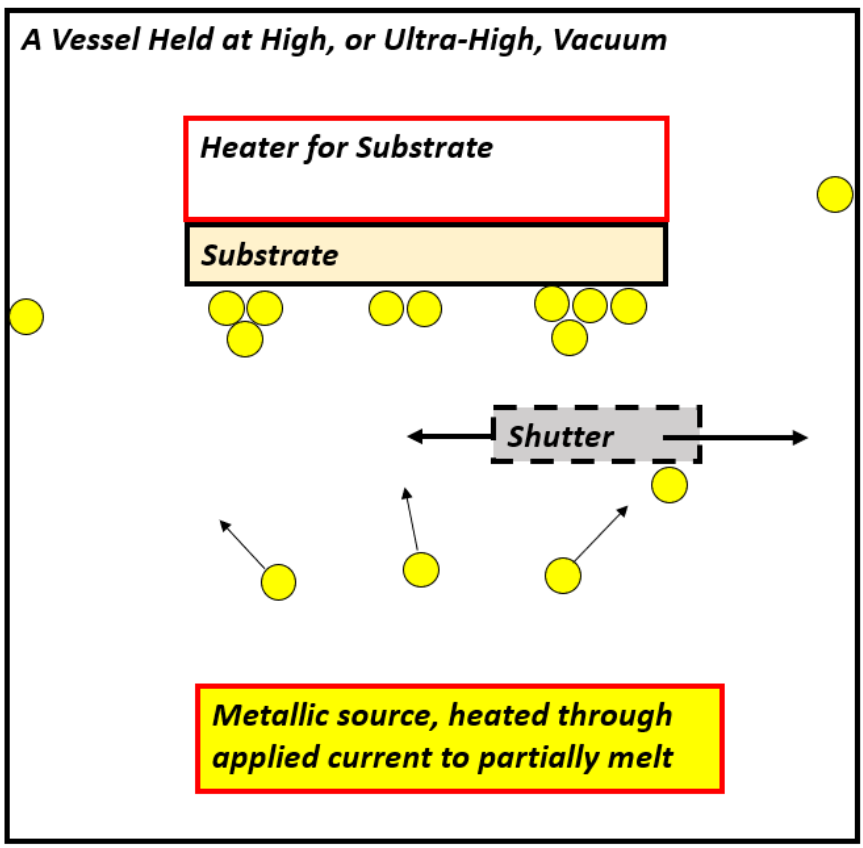

Figure 1: An illustration of what a very simple thermal evaporation deposition system might look like. This includes the shutter, which is necessary to manage how much of the deposition reaches the substrate.

The substrate's temperature can range as high as 1000° C [5], which poses an interesting de-

sign constraint, as unaccounted for heat within the system can induce outgassing, the release of gasses otherwise dissolved within solids. These gasses severely impinge upon the quality of a deposited thin film and must be accounted for, through adequate pumping or outright prevention whenever possible. The standard heating setup can make the management of heat difficult, however, due to the inefficiencies of conduction in vacuum. As seen in figure 2, traditional heaters are throttled by the small surface imperfections between mated surfaces which reduce the area of effective conductive contact. Trials where the substrate is ineffectively affixed to the heater can fail, with uneven crystal growth and poor adhesion between the film and the substrate, thus wasting time and resources within the lab.

Designing around the problem of ineffective heaters was a major guiding force in this design's proposal. By adding a secondary heater, the limitations of the conductive contact can be overcome, through effective radiative heating. This requires a significant amount of additional infrastructure within the chamber, so by integrating multiple necessary components into this single design multiple issues can be solved with a singular composite system, providing a means to significantly improve the quality of produced thin films. Figure 3 below shows what this system might look like in more explanatory detail. Note how the water cooling needs are directly incorporated into the walls of the structure which encloses the heater, allowing the heat very little space to escape from. Note also how the bottom heater, insulation, and water cooling are all a part of the shutter, which has already been discussed as a requisite piece of equipment. Figure 4, in contrast, shows what the final assembled design looks like within the 3D computer aided design (CAD) software used, Autodesk Inventor. Note how the enclosure of Figure 3 correlates to the copper block seen at the center of Figure 4.

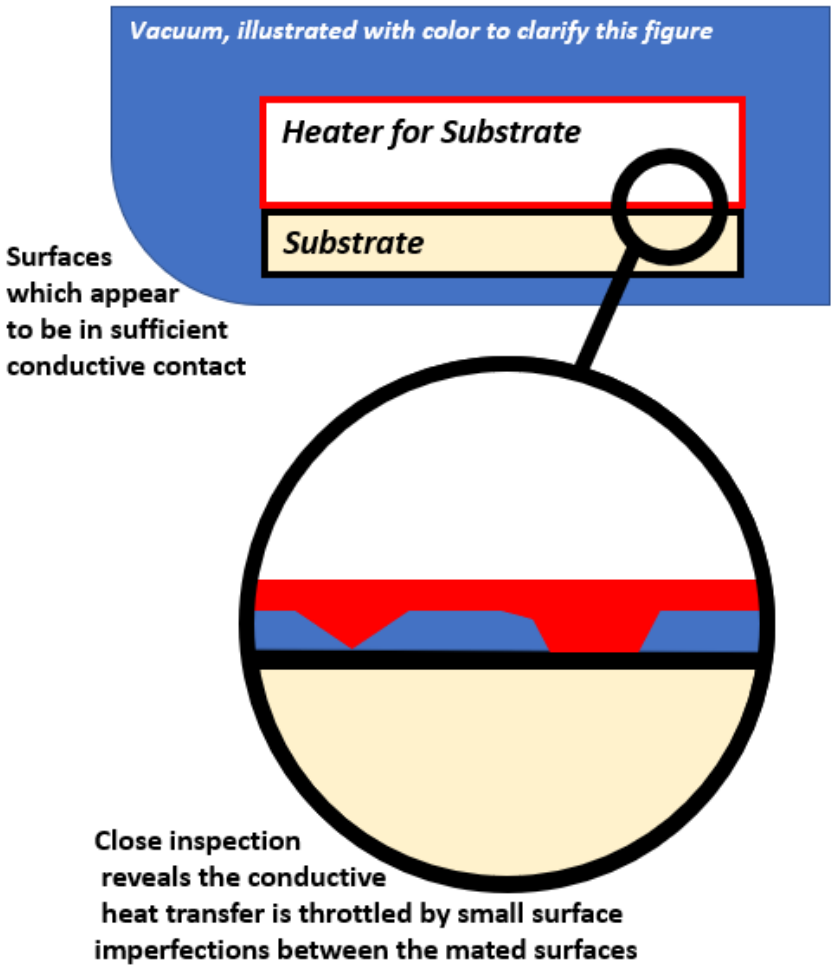

Figure 2: An illustration showing the way mated surfaces can be in imperfect conductive contact while under vacuum. Notably, the substrate is shown as perfectly flat, but this is because the Bumm group's substrate of choice, mica, cleaves to atomically flat surfaces.

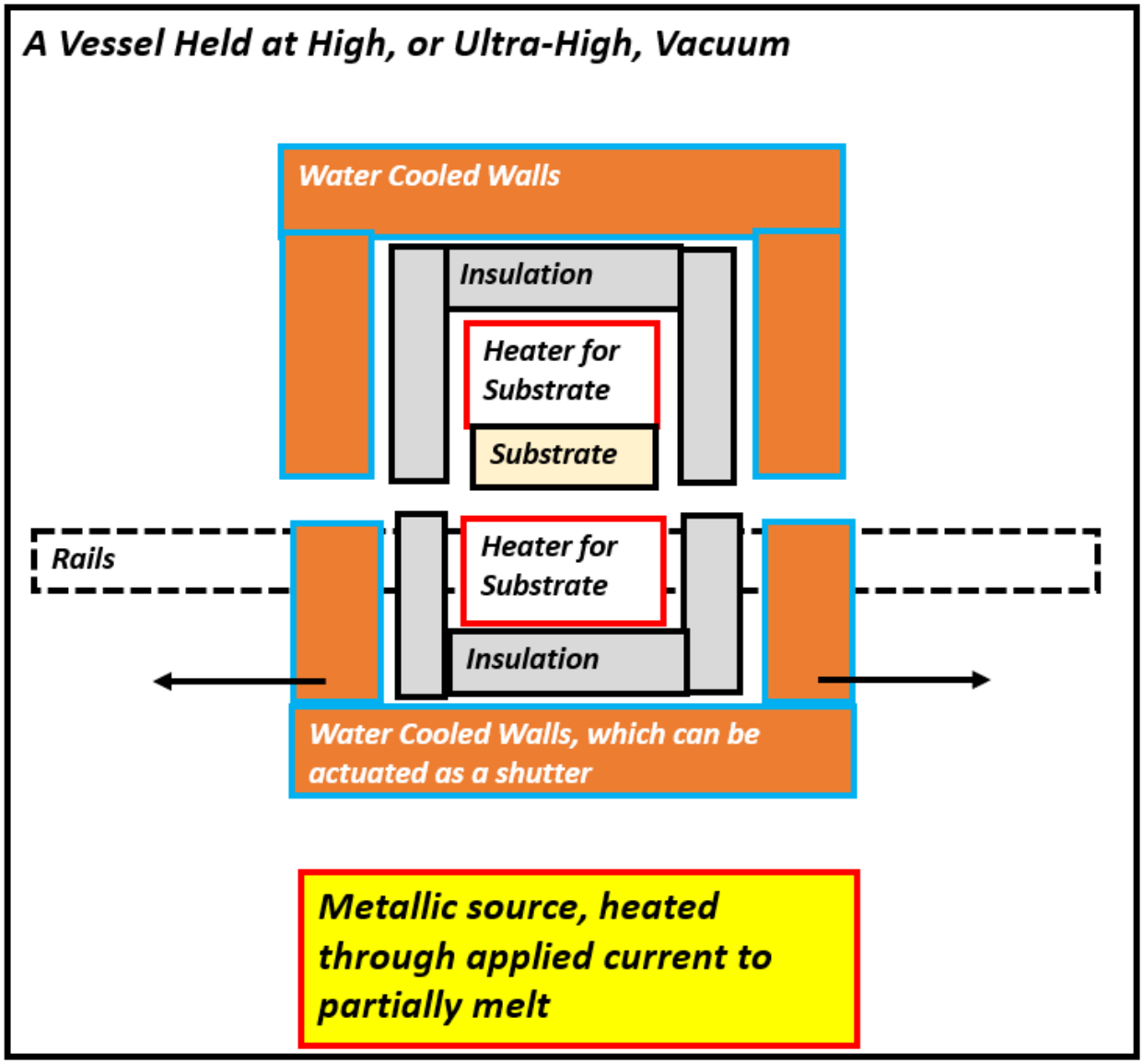

Figure 3: A very simply presented form of the heater and integrated equipment proposed, with labels denoting what each color-coded piece represents.

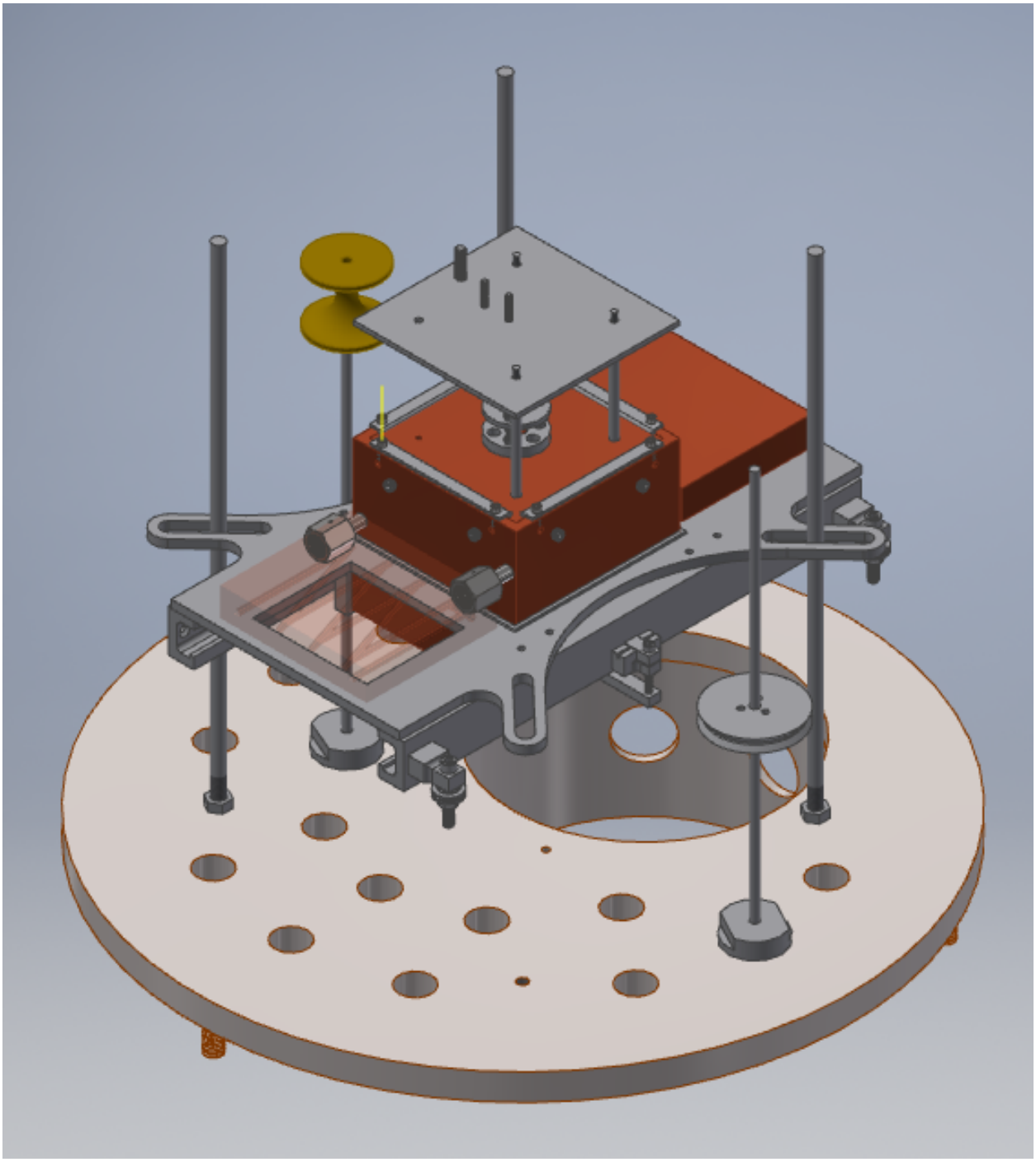

Figure 4: A CAD rendering of the components designed and the base they are installed onto.

2.1 Water-Cooled Walls

Almost all of the system's components are encompassed by the thick copper walls which make up the outside of the 'box'. The high thermal conductance of the copper makes it ideal as a sink material to remove unaccounted for heat in the system. Additionally, copper's machinability means that more complicated manufacturing operations can be employed, and special capabilities can be utilized in the final design.

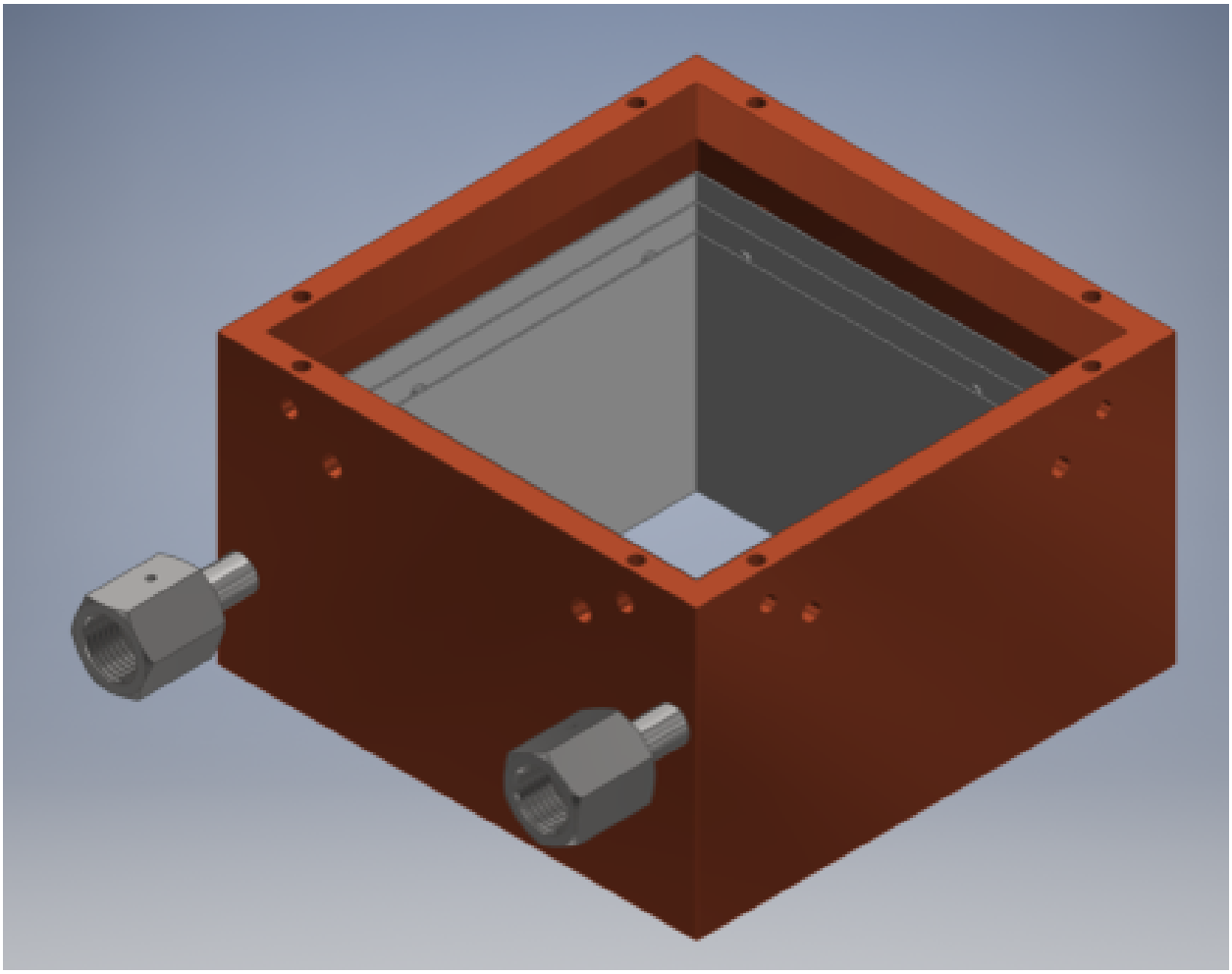

Figure 5: The 3D model of the heater's walls, the insulating tantalum sheets, and the brazed VCR fittings which connect to the internal water lines.

This design, seen in figure 5, employs a significant amount of cooling through the use of stepped waterlines made by through holes drilled in the center-line of each wall with plugs affixed to the

entrance and exit holes. This water removes the escaped heat of the ceramic heaters, preventing that heat from leaking into the rest of the chamber. These walls can be more clearly seen in figure 6, which also isolates the walls from the sheets of tantalum and fittings. The fittings are simply commercially available VCR® compliant butt-welded plugs, with a retained nut. These fittings are a common choice when sealing fluid lines inside a high vacuum, as water leaked into the chamber has the potential to damage, or destroy, many of the other components. Thus, VCR® fittings are necessary, as their made-for-vacuum seals utilize compressed metal gaskets and thus offer a very compliant seal. The choice of fittings further elaborated upon in section 3.2.

A discussion of the methods used to calculate the needs of this system is found in section 4.2, and the CFD modeling techniques used to validate this design is the subject of chapter 5.

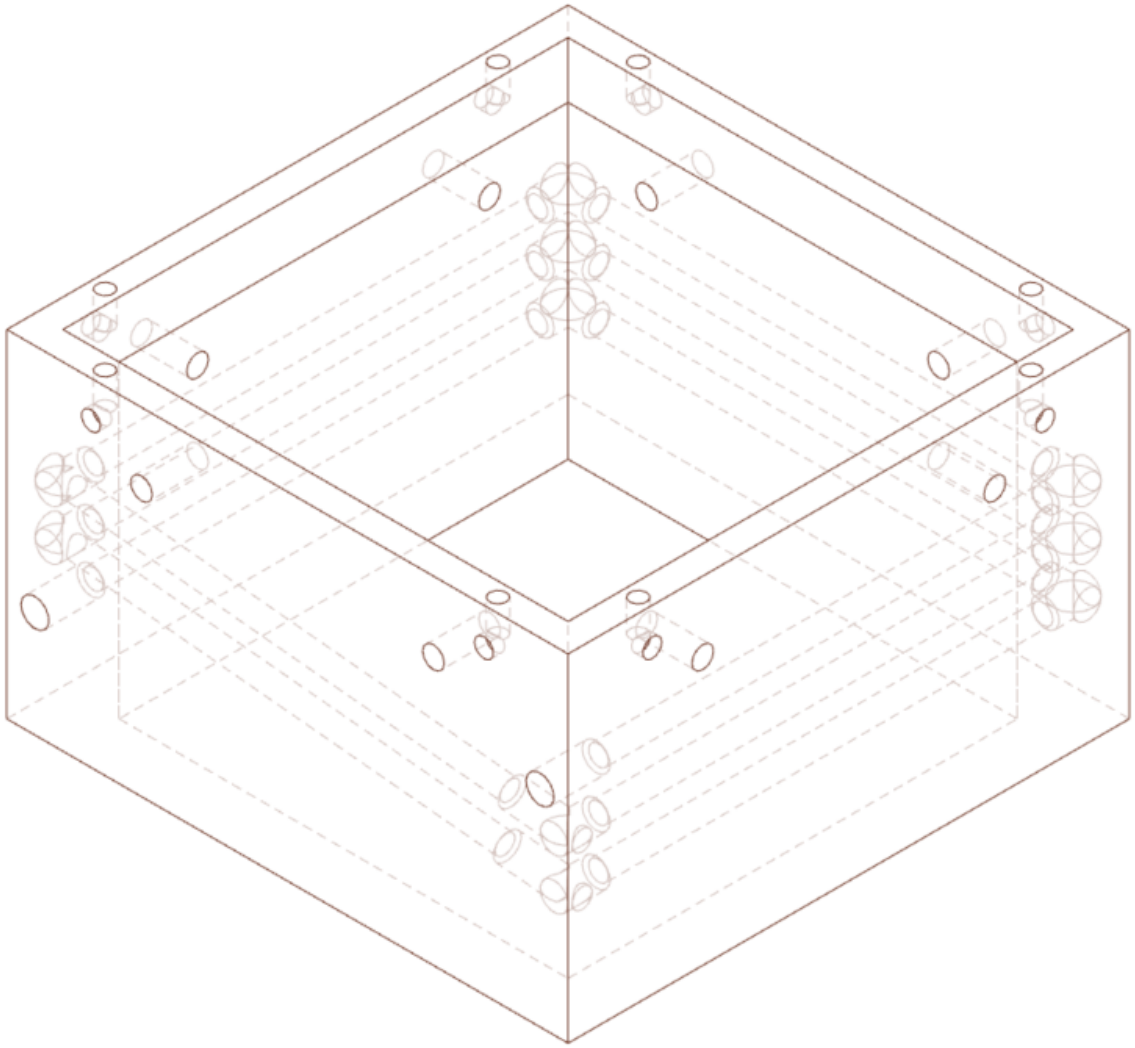

Figure 6: The 3D model of the heater's walls, with transparency enabled such that the water-cooling lines are visible.

2.2 Lid

A priority of this design has been ensuring the ease of use for the end user. This means that it needs to be as simple and quick as possible to replace the substrate, once the desired film has been deposited and collected. This system addresses that need by mounting the substrate holder to the lid of the setup, so that a user can simply pick up, invert and remove the lid from the chamber to have free, unencumbered access to the substrate. This can be seen illustrated below, in figure 7. Note that this sketch doesn't account for the hardware necessary to retain the actuated heat-sink, which would come later in the design process.

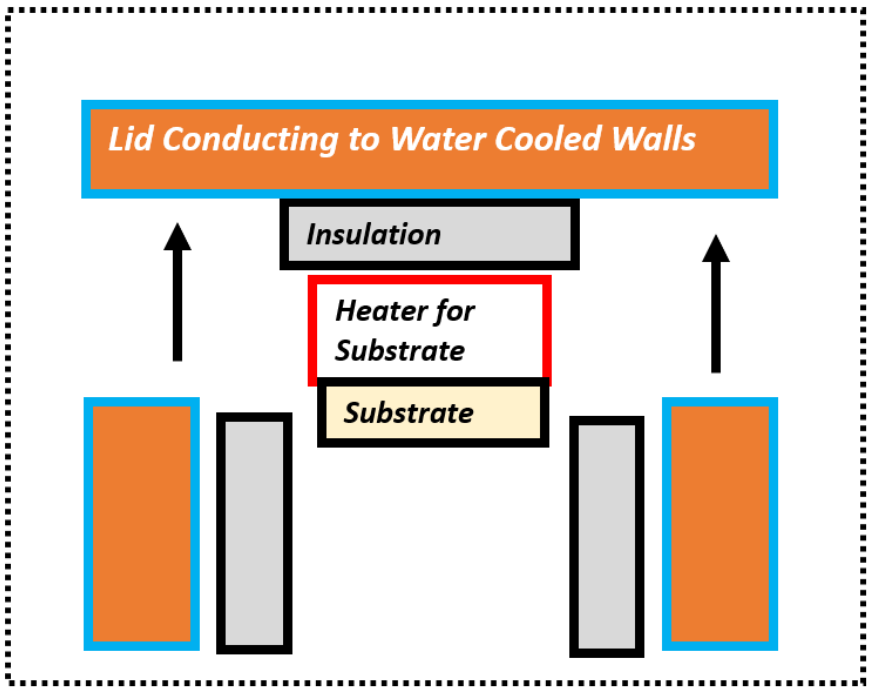

Figure 7: An illustration of the way the lid was intended to be separated from the rest of the equipment, to ease access to the substrate.

And on the underside of this lid, seen in figure 9, there are layers of tantalum for insulation, and the mounting hardware for the alumina block, and finally the alumina block itself. The alumina block will have tungsten-rhenium heating elements within, to facilitate the actual heating of the substrate. The desired substrate will be clipped onto the block, and the block will be secured through bent wires, to reduce heat lost due to conduction into the rest of the assembly. The lid

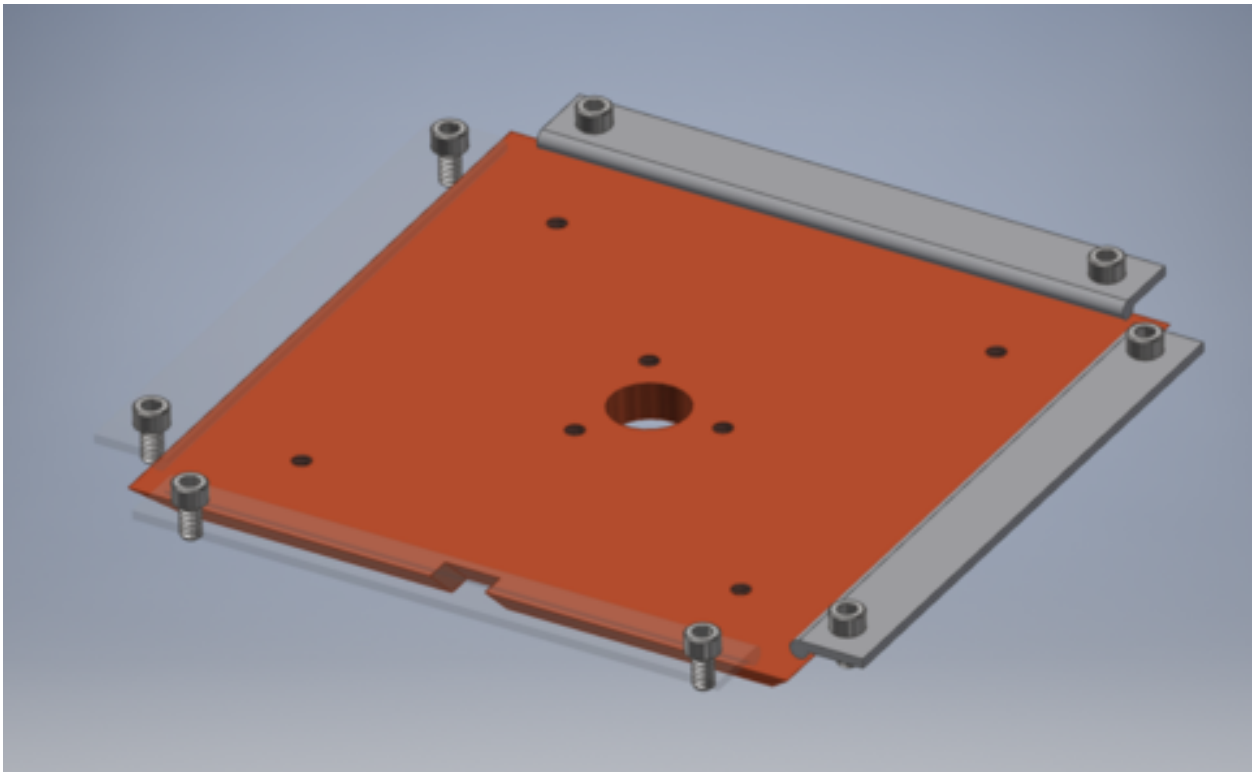

Figure 8: The heater's lid, isolated from the rest of the CAD assembly

contains a slot within the lip which is sized to ease prying the lid off the box's top. The lid also features a hole in its center, to accommodate the actuated heat-sink, which is discussed in the following section. Of further note is the retaining hardware seen on each of the lid's four sides. The bolts screw into threaded holes within the topmost face of the walls, and allow the user to tighten the hardware between the lid and the bolt's cap. In this way, the user can lighten the connection between the lid and the walls, through the bolt's compression, which is distributed by the bar affixed by both bolts. The bar acts to distribute the load applied by each bolt. However, alternative designs have been provided which use the bolts as point loads, in case the bar method proves too cumbersome for regular use. A bar which can be slid on or off the retaining bolts has also been designed as a less complex solution, however it could potentially slip during tightening and prove itself more of an annoyance than a solution.

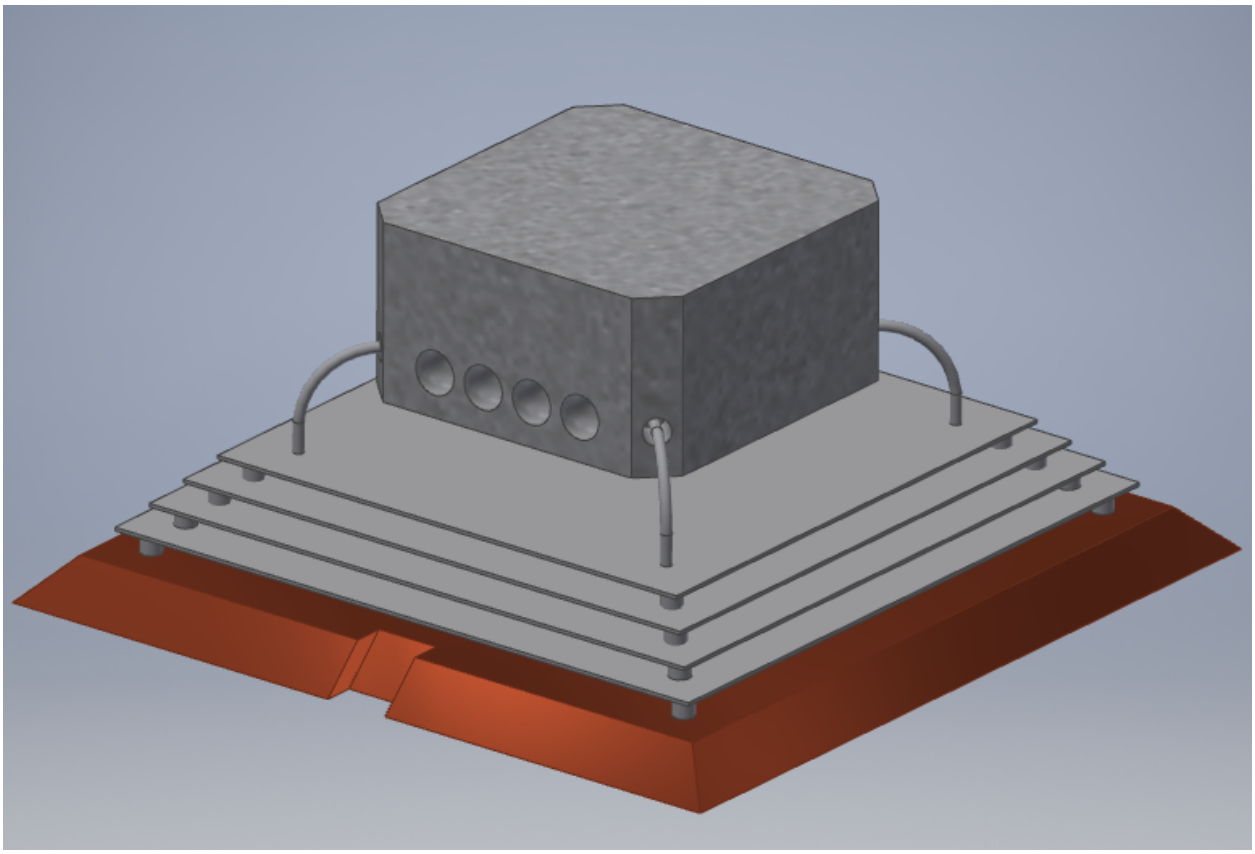

Figure 9: The underside of the heater's lid, isolated from the rest of the CAD assembly

2.3 Actuated Heat-Sink

Every aspect of this design focuses on improving the usability for thin film deposition, and that includes improving the duty cycle of the setup. The heat sink's role is to hasten the cooling process once a deposition has completed, by providing a highly thermally conductive path from the alumina heating block to the water-cooled exterior walls. Without this component, one would have to wait up to several hours for all of the heat to safely dissipate from the heater's interior, due to the design's insulating properties. This heat sink gives the operator a shortcut, offering the heat a direct conductive path from the alumina to the copper exterior, and better yet the heat wicking water lines. An illustration of what this might look like is seen below, in figure 10. Actuating this heat-sink presents a challenge due to the constrained space and the properties of vacuum.

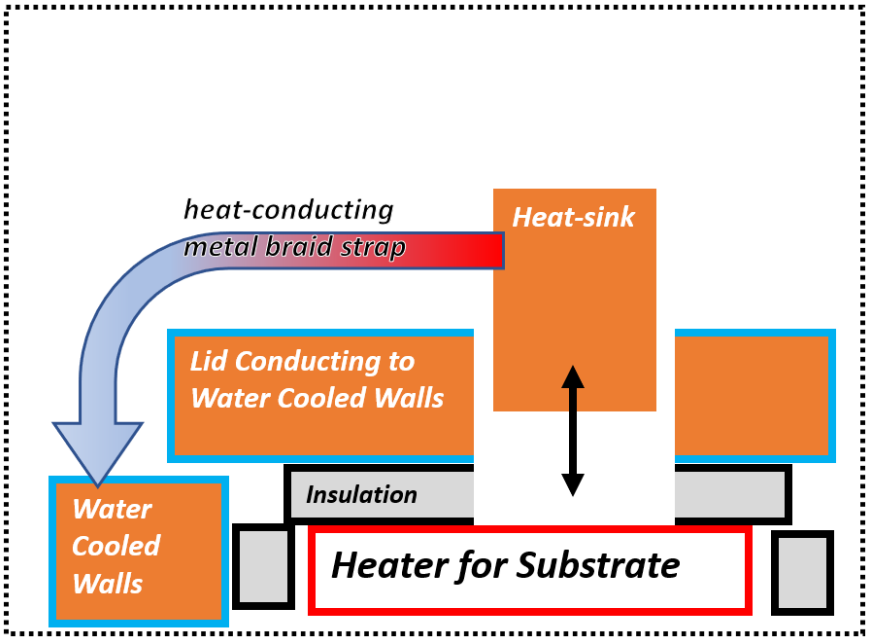

Figure 10: A simple presentation of how an actuated heat-sink could be manipulated to touch, or not touch, the alumina heater.

In atmosphere, oftentimes what appears to be conductive heat transfer is heavily supplemented by a conductive layer of air; this means that, while two bodies may appear to be touching, the surface area in contact may be very small as discussed in the beginning of this section. In the

instance of this conductive heat-sink case, there's an apparent need to align two axes in three-dimensional space, that of the alumina's top face and the bottom face of the cylindrical heat-sink, to achieve the highest quality contact. It's less important to achieve perfect contact here than in the case of substrate heating, as quickening the cooling process merely shortens the time one must wait to access the chamber, but the spring is still necessary because of the potential for askew faces to have a notable gap between them, like a can which has begun to tip over. To compensate, our actuation scheme takes advantage of the compressive force of a spring, aligning the face of the heat-sink's cylinder to the top-most face of the alumina through an equalized distribution of force, as the spring attempts to maintain the alignment of its top and bottom faces. This force maximizes the conductive area, and thus the heat conducted out of the block.

Much like an active high switch, when the spring isn't displaced it presses the solid cylinder of copper, the sink, against the alumina, the source. Were this actuated with a solid rod mounted onto a linear feedthrough, one might accidentally push the heat-sink too firmly into the alumina, cracking it. By actuating this setup with a cord, the compressive tension of the spring defines the force between the heat-sink and the alumina, and this force is adjustable through the tightening or loosening of the topmost circular plate's retaining bolts. It also simplifies the process of uncoupling these actuation pieces when the lid needs to be removed for accessing the substrate.

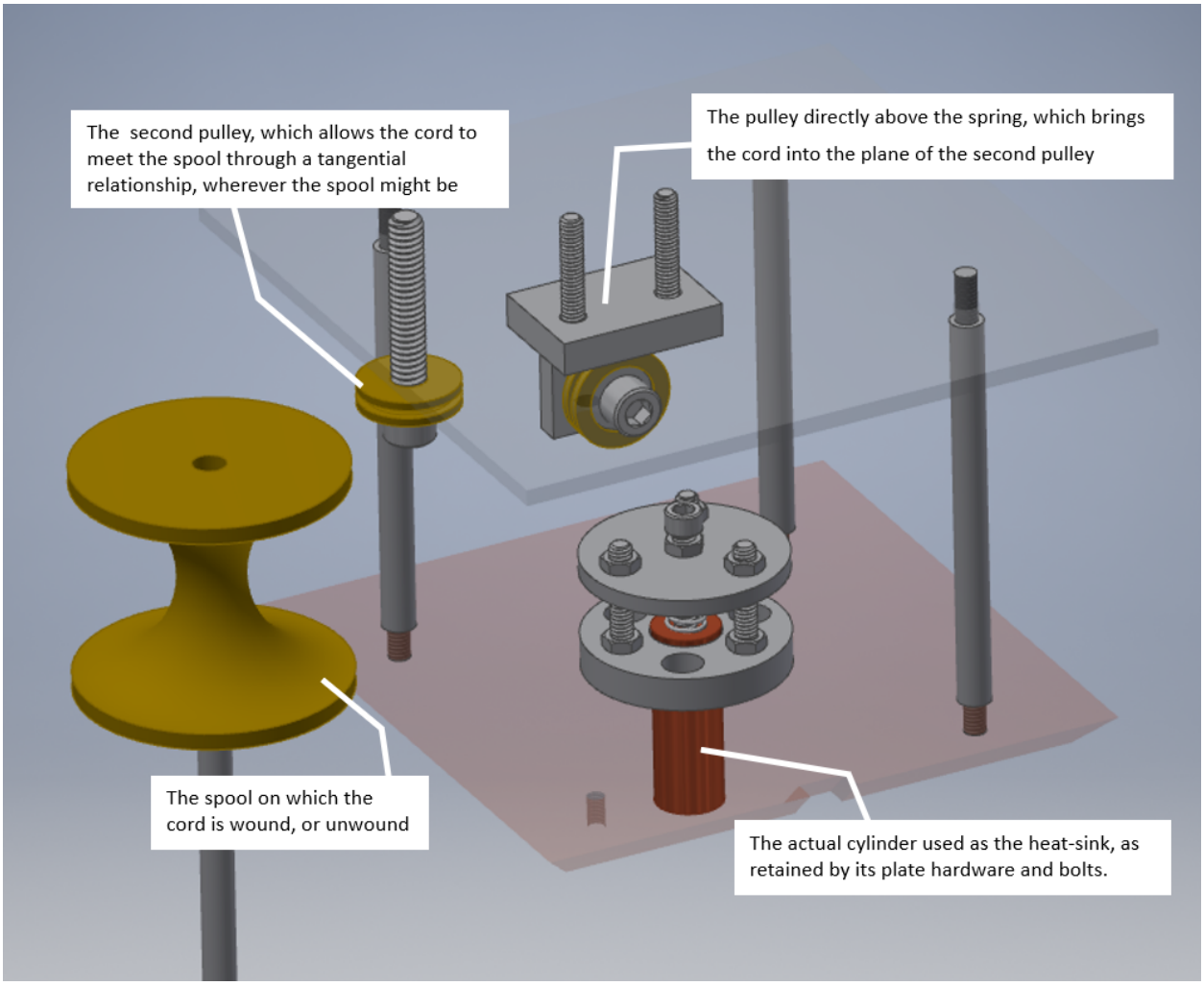

Figure 11: The model for the assembly of the actuated heat-sink. The heat-sink itself can be seen as the copper cylinder at the bottom of the image.

2.4 Shutter-Cart

The traditional shutter of vacuum setups is the basis of a surprising number of components. This is at least partially because by its simplest definition, a surface which can be manually moved in-and-out of the way of the deposition source, a shutter can accomplish the vast majority of desired operations. The simplest shutters allow technicians to precisely control the amount and quality of adsorbed material, by preventing deposition until a steady flow is achieved and only allowing deposition for the desired amount of time, thus controlling the number of layers. In a similar respect, by placing an electrified quartz crystal on a shutter one can measure the deposited material by the damping of the quartz's vibrations as its mass increases with deposited material and interpreting the resultant flux. This shutter's design exists in contrast to those most widely available, most importantly because of its integration of a heating element.

The bottom shutter is essentially a mirrored and compressed version of the system lying above it. This is another utility-minded choice. A totally passive shutter would only maintain a barrier between the evaporating source and the adsorbing substrate. This barrier allows the operator to finely control the amount of deposited material in the thin film. However, it does nothing else.

Instead of relying on a layer of fluid to facilitate effective heat transfer, this design emphasizes the radiative application of heat to the substrate. While the substrate is affixed to the top ceramic tightly to provide some conductive transfer, the Shutter-Cart's heater's radiative heat substantially compensates that which is provided by the above heater. In this way the substrate is hopefully brought to the desired temperature, and an equilibrium, in a more uniform manner, which provides a surface that better facilitates the growth of large, continuous, flat metallic crystals.

Starting from the outside and working in on the assembly seen in figure 12, the copper walls function similarly to those of the top, allowing a reservoir for remnants of escaping heat, though the cooling lines to remove this heat are within shields mounted above where the cart is displaced to when it isn't shielding the substrate. Then layers of tantalum insulate the heater from radiative heat losses, reflecting that heat back at the heater to help it build in temperature. Finally, a dupli-

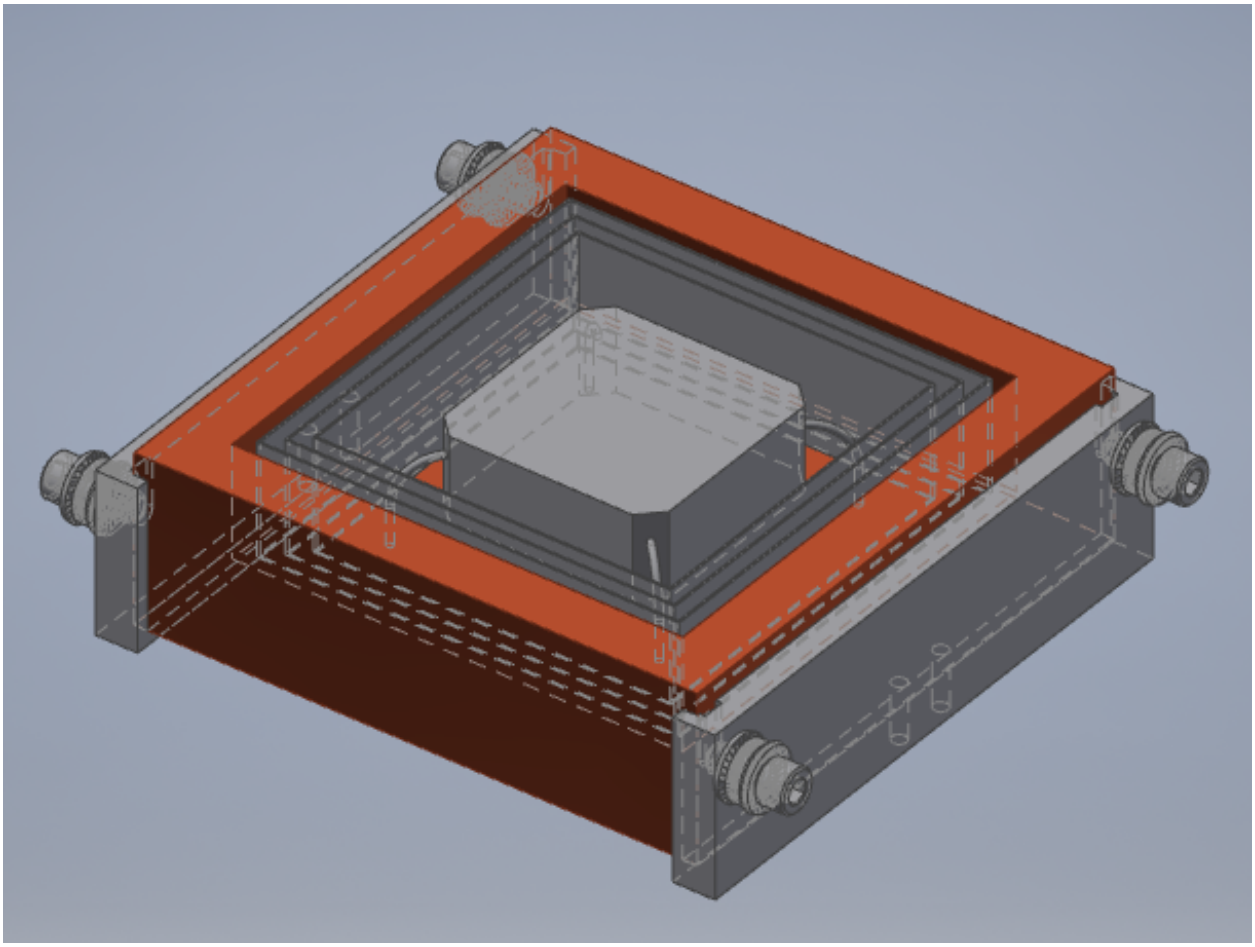

Figure 12: The shutter-cart, as modeled. At each of the four corners there's a bearing which is fastened such that it can freely rotate, and act as the "wheels" of the shutter-cart.

cate alumina heating block radiates heat directly at the substrate above. Of course, all of these components contribute to the overall weight of this piece of the system, the shutter-cart's copper will weigh about 7 pounds and the alumina alone weighs almost half a pound. Section 3.5 further elaborates on the weight considerations.

2.5 Rails

The complexities of this heater design bely a much greater effectiveness of the system as a whole, but the benefits do come at significant costs. One of the largest design sacrifices made was that of weight. While an ordinary setup's shutter could weigh mere ounces, ours weighs nearly 7 pounds, over 3 kilograms. This is a trivial amount when manipulated outside the chamber, but when hung above thousands of dollars of equipment within a sealed container at vacuum, it's another proposition entirely. Those traditional shutters are actuated using rotary feedthroughs, rotating the shutter between the source and substrate when so desired. But by creating a dramatically heavier shutter, the rotary feedthrough's limitations are exposed. Rotary feedthroughs have maximum axial loads, and the torque necessary to actuate the shutter is greatly effected by the weight of the given shutter. Therefore, instead of mounting the shutter on a rotary feedthrough, the entire shutter is mounted to a cart which is free to smoothly ride along rails, using bearings as wheels. This takes the weight off the rotary feedthrough, and makes the required torque a function of the feedthrough's performance as a pulley rather than the weight of a given shutter. Additionally the pulley's performance can be improved, should it prove an issue, in contrast to solving issues when mounting directly to a rotary feedthrough, where the choice of solutions essentially comes down to removing equipment borne by the feedthrough or buy a new feedthrough entirely. The rails rest on the overall support frame for the heater so the weight of the shutter-cart is borne by the four mounting rods which are fastened to threaded holes in the chamber's base. The overall support frame also incorporates shields which prevent the shutter's heat from reaching the bell jar when displaced from under the top heater, which is also supported by this frame.

In designing this way, the shutter will always be supported, no matter what systems might break. Additionally, this strictly dictates the motion of the shutter, giving the operator precise and rapid control along the length of track.

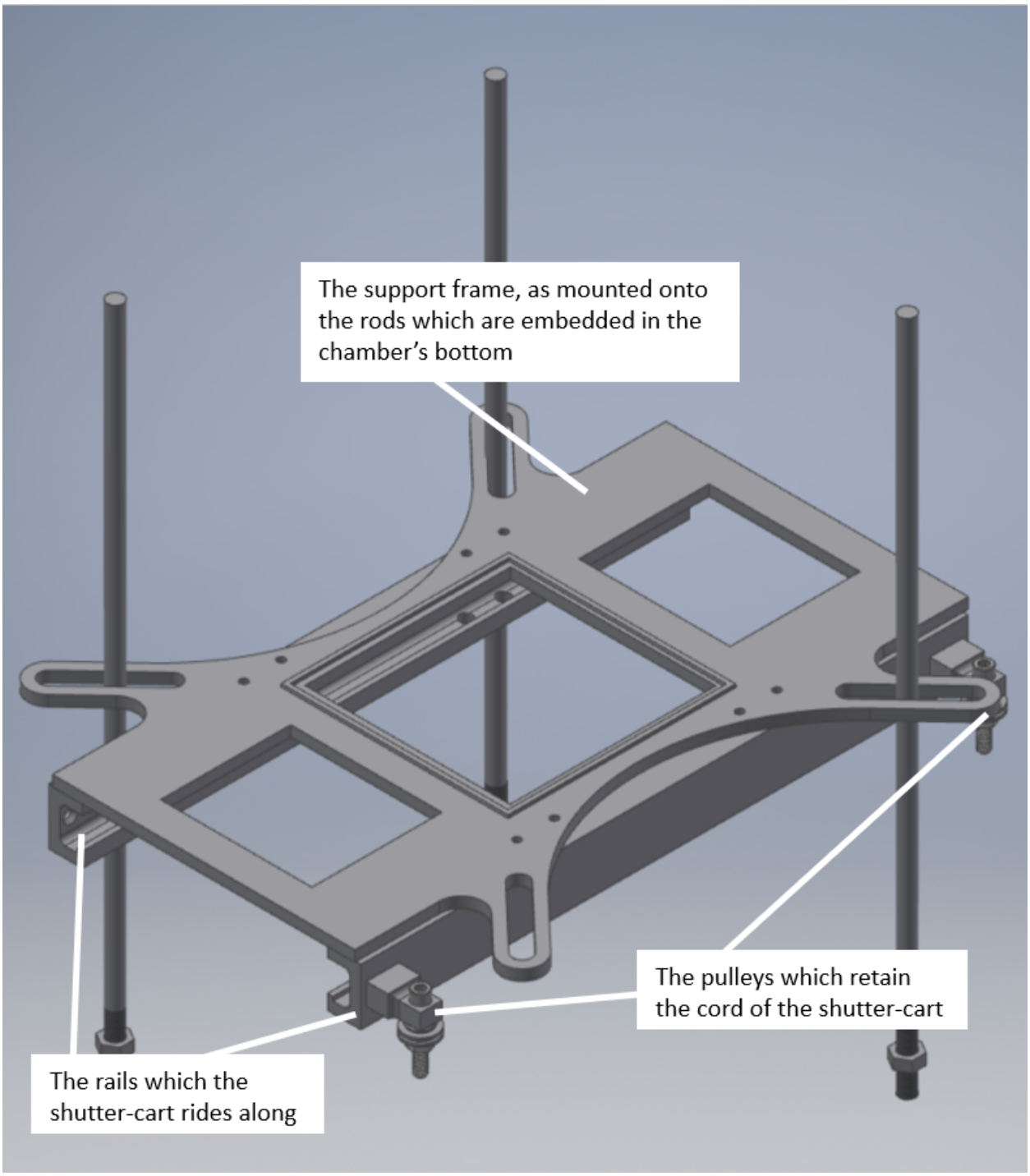

Figure 13: The rails and their associated structures, the plate which the heater rests upon and the posts which carry the entire structure, with two posts omitted for visual clarity.

2.6 Actuation

Actuation within the chamber became a huge cause of concern as the project went on. At least two components of the heater assembly needed to be movable from the outside. Each proposed solution came with benefits and drawbacks which needed to be compared in order to decide upon an agreeable solution. While certain off the shelf solutions addressed these needs, their prices increase exorbitantly with their capabilities. An effort has been made to reuse existing equipment, and as such designs which relied on the rotary feedthroughs in the Bumm group's possession were given priority over designs which might use linear feedthroughs that would need to be purchased.

When considering actuation options it's important to consider that many solutions for transferring mechanical power and motion in atmosphere are inappropriate under vacuum. The friction of most gears can cause particulates to loose and additional offgassing surfaces to be exposed, heat can be conducted or stored in troubling ways, lubricants and other coatings are often sources of significant off-gassing, and commercial alternatives of all of these subjects come at a premium when purchased to accommodate maintaining the vacuum's cleanliness. A compromised choice was made, then, to design actuating equipment which integrated just one specialty vacuum-safe part, ultrahigh vacuum compliant bearings sold by MDC Vacuum. These radial bearings are designed for specialty actuation applications within ultrahigh vacuum, are not enclosed and thus cannot contain pockets of air, and utilize a proprietary vacuum compliant lubricant, in lieu of the machine oil which would be used for standard machine bearings [2].

Chapter 3

Mathematical Analysis

3.1 Radiative Heat Transfer Calculations

This step of the thermal evaporator design process is to create an effective substrate heater. The heater's effectiveness is to be evaluated based on how evenly it provides a 1000 ° C face of an alumina block, with dimensions of approximately 3 × 3 inches, which our substrate will rest upon; and how efficiently it uses its supply power to reach this temperature.

Simplified analysis began with an assumed shape of an alumina block, 3 × 3 × 1 in, with a surface area of 30 in^2 (0.0193548 m^2), heated to a steady-state (isothermal) of 1000 °C (1273.15 K). We will initially treat this shape as a sphere of equivalent area.

Using this first rough assumption, we can calculate the approximate power radiated from an akin blackbody using the Stefan-Boltzmann law (1).

$$P = A\sigma T^4 \tag{1}$$

Where

$$\sigma = \frac{2\pi^5 k^4}{15c^2h^3} = 5.670373 \times 10^{-8}\ \mathrm{Wm^{-2}K^{-4}},$$

$P \equiv$ Power Radiated, W

$A \equiv$ Surface Area, m^2

$T \equiv$ Absolute Temperature, K

This initial estimate offers

$$P \approxeq 2889\ \mathrm{W}$$

This heat loss indicates that we would need to supply that level of wattage to maintain the desired temperature of the block at steady state. Any unaccounted for heat loss has the potential to negatively impact the quality of the deposition, or heat something else in the chamber; every

accounted for watt, at steady state, needs to be removed from the system. Thus, minimizing the required wattage minimizes the required cooling, which minimizes the risk of cooling related failure. This failure is why the estimate needs to be accurate, or at the very least excessive.

The first refinement to make is to assume a nonzero environmental temperature, as it's unlikely the chamber will be kept at 0 K. Instead, a more reasonable assumption is that the chamber will be at equilibrium with the temperature of the lab, which is inside an air conditioned building. Therefore, the approximation will use 25 ° C for the surroundings, standard ambient temperature,

$$P = A\sigma\left(T_{\text{body}}^4 - T_{\text{surroundings}}^4\right). \tag{2}$$

This only reduces the required heat to 2,875 Watts.

Treating the heater and the chamber walls as objects with arbitrary geometry, instead of formless concepts, can help narrow down the actual expected wattage. Using what's called the shape factor, or view factor, F_{i-j}, for bodies i and j is the first step in understanding the importance of the physicality of the surfaces, that is, that they exist as physical objects whose geometry and spatial relationships can influence how effectively the heat is transferred. For example, two surfaces facing opposite directions cannot radiate heat between themselves.

These are only functions of geometry, and act as coefficients to the terms in the black body emission calculations (3).

$$\dot{Q}_{1-2} = A_1 F_{1-2}\left(E_{b1} - E_{b2}\right), \quad E_{bi} = \sigma T_{bi}^4 \tag{3}$$

In the case of a body fully enclosed by the surface of another body, like our approximation as it currently stands, or a pair of concentric spheres, the view factor is $F_{1-2} = 1$, as all emitted radiation is captured by the enclosing surface. This level of approximation does not account for what fraction of emitted radiation reaches the surface which emits it, F_{i-i}. For the case of two infinite parallel planes, this is zero. But for 2 concentric spheres, per our approximation, this is a nonzero fraction. Because the sheets of tantalum and other faces cannot self-reflect, as they do not have

the curvature, it is more helpful to approximate these shapes using sequential planes of infinite area, rather than concentric spheres. This will be the solution method moving forward, albeit with solutions that incorporate the area, rather than the heat flux results which are more commonly used in 'infinite plane' approximations.

The next assumption is that sheets of tantalum will be used to reduce the radiative losses of the block, as this is a standard insulating material in alike applications. In conduction analysis there's a concept of thermal resistance, in analogy to electrical resistance, to calculate the reduction in heat transfer in a system due to the presence of a given material. Though this approximation is far from accounting for whatever conductive heat transfer may occur, this technique can still be used to better calculate the radiative heat losses. Before accounting for the emissivity constants, ε, and treating the block as being fully shrouded by the sheets, then again shrouded by the chamber walls, it's obvious from the zeroth law of thermodynamics, that of equilibrium, that the tantalum sheets must reach a temperature between that of the surroundings' sink, and the block's source. In this approximation (before accounting for the emissivity values), every nth sheet reduces the heat losses by a coefficient of $\frac{1}{1+n}$ [3].

$$P = \frac{1}{1+n} A\sigma T^4 \tag{4}$$

With this coefficient in mind it's trivial to determine the substantial efficiency gains the sheets provide. However, once one accounts for the emissivity values, the sheet's insulating efficacy is reduced. In the continued effort to solve for overestimates of the required power, these emissivities must be accounted for.

Emissivities are an important part of how effectively materials radiate heat. These coefficients, represented with ε, work alike to the view factor, except they're independent of the final geometry. They're merely functions of what materials each body is made of, and sometimes what temperature as well. This analysis will use the upper limits of these values, so that the approximation favors overcompensating, thus accommodating the upper limit of the system's requisite power.

Pulling from a table compiled by the Mikron group [9], we have a number of applicable emis-

sivities.

$$\begin{aligned}\varepsilon_{Al_2O_3} &= 0.42\\ \varepsilon_{Ta} &= 0.26\\ \varepsilon_{Cu} &= 0.88\end{aligned}$$

For our two body, heater and surroundings, case, this modifies equation 1 such:

$$P = \varepsilon'\sigma A(T_{\text{body}}^4 - T_{\text{surroundings}}^4) = 1,142\,W, \quad \varepsilon' = \frac{1}{\varepsilon_{Al_2O_3}} + \frac{1}{\varepsilon_{Cu}} - 1 = 0.3972 \tag{5}$$

This accountability has already halved the initial expected wattage, without accounting for insulating layers. Continuing, here's an equation accounting for the decreased wattage per added layer. Note that this is still an approximation using arbitrary parallel planes of identical area, including the planes of the shield layers.

$$P = \frac{\sigma(T_b^4 - T_s^4)}{R_b + R_1 + R_2 + \cdots + R_i + \cdots + R_n + R_s}, \qquad \begin{aligned} R_b &= \text{Resistance of the emissive body, } \tfrac{1-\varepsilon_b}{A\varepsilon_b}\\ R_i &= \text{Resistance of the individual shield(s), } \tfrac{1}{A} + \tfrac{1-\varepsilon_i}{A\varepsilon_i}\\ n &= \text{The Number of shields being used}\\ R_s &= \text{Resistance of the surface, } \tfrac{1}{A} + \tfrac{1-\varepsilon_s}{A\varepsilon_s}\end{aligned} \tag{6}$$

We can simplify this equation significantly by expecting the shields to be made of identical mate-

rial,

$$P = \frac{\sigma(T_b^4 - T_s^4)}{R_b + R_1 + \cdots + R_n + R_s}, \qquad \begin{aligned} R_b &= \text{Resistance of the emissive body, } \tfrac{1-\varepsilon_b}{A\varepsilon_b} \\ R_{\text{shield(s)}} &= \text{Resistance of the shield(s), } \tfrac{1}{A_i} + \tfrac{1-\varepsilon_i}{A_i\varepsilon_i} \\ n &= \text{The number of shields being used} \\ R_s &= \text{Resistance of the surface, } \tfrac{1}{A} + \tfrac{1-\varepsilon_s}{A\varepsilon_s} \end{aligned} \tag{7}$$

Substituting in the desired values to (7), and using the simplified assumption that all of the insulating layers will have the same surface area as the alumina block, the respective values are

$$P = \frac{\sigma(T_b^4 - T_s^4)}{R_b + n \cdot R_{\text{shield(s)}} + R_s}, \qquad \begin{aligned} R_b &= \tfrac{1-\varepsilon_{\text{Al}_2\text{O}_3}}{A\varepsilon_{\text{Al}_2\text{O}_3}} = 71.35 \text{ m}^{-2} \\ R_{\text{shield(s)}} &= \tfrac{1}{A} + \tfrac{1-\varepsilon_{\text{Ta}}}{A\varepsilon_{\text{Ta}}} = 198.6 \text{ m}^{-2} \\ n &= \text{The number of shields being used} \\ R_s &= \tfrac{1}{A} + \tfrac{1-\varepsilon_{\text{Cu}}}{A\varepsilon_{\text{Cu}}} = 7.0 \text{ m}^{-2} \end{aligned} \tag{8}$$

Putting these values into table 2 seen below, it's evident that the insulating layers provide dramatic returns on heating efficiency, but that those returns do diminish.

Number of layers	Expected Wattage	Wattage decrease
0	1895	N/a
1	536	−1359
2	312	−224
3	220	−92
4	170	−50
5	138	−31

Table 2: The anticipated wattage to maintain 1000 ° C for a given number of tantalum layers, and the subsequent reduction in wattage each additional layer facilitates

This approximation has yet to account for the necessary increase in area each enveloping surface must accommodate, since parallel planes may all hold identical areas, but spheres encompassing one another must get progressively larger. This will decrease the required power of the approximation, as is evident from the surface area variable in the resistance terms of (6), (7), and (8).

3.2 Water Flow Heat Transfer Calculations

The first step in calculating this system's rudimentary cooling needs is to use a steady-flow energy balance equation.

$$\dot{Q}_{in} + \dot{W}_{in} + \sum_{in} \dot{m}\theta = \dot{Q}_{out} + \dot{W}_{out} + \sum_{out} \dot{m}\theta \tag{9}$$

Many of these terms can be eliminated off the cuff. The only energy introduced is the heat, $\dot{Q}_{in}$, of the heating element, and the kinetic energy and work done by the cooling line is negligible, leaving only $\dot{Q}_{out}$. From the sections 3.1 calculations it can be assumed that less than 600 W of power will be used to heat the alumina, so this will be used as an overly safe upper bound on the heat which needs to be removed from the system. Lin Hall is equipped with chilled water lines to supply the cooling needs of the building's equipment, so this is our chosen cooling fluid. Because these lines were designed to support multiple applications of similar scale, their limitations will not need to be considered, as later analysis will prove.

Moving forward with these simplifications, we get the following form,

$$\dot{Q}_{in} = c_{p,avg}\,(T_{outlet} - T_{inlet})\,\dot{m} \tag{10}$$

Because the cooling system is oversized, the outlet temperature of the water will be kept to a minimum of 10 °C above the inlet, rather than maximizing the cooling potential of the water. Solving this equation provides an $\dot{m}$ value of 14 g/s, which given the density of water is 14 cm^3/s or 0.84 L/min. To simplify further calculations this will be rounded up to 1 L/min. This volu-

metric flow rate will be used moving forward.

The next design choice was to pick an appropriate VCR fitting for the given thickness of the copper walls. The corresponding pipe diameter will determine the cross-sectional area of the fluid at any given point, and thus determine the flow velocity. This is an important quantity, as it will later help determine the Reynold's Number, and thus the measure of turbulence within the pipes. The more turbulent the flow, the better the heat transfer, as more of the fluid is exposed to the outer walls. The Reynold's number also depends on the fluid density, dynamic viscosity, and hydraulic diameter of the line. The hydraulic diameter is the same as the line diameter, so it's also dependent on the choice of VCR fitting. All of these factors were tabulated, then correlated to the pressure drop each line would experience. While it's expected that Lin Hall's chilled water will be sufficient, the variables at play correlate to magnitudes of difference, and higher pressure systems hold higher risks in vacuum. The Haaland equation

$$\frac{1}{\sqrt{f}} = -1.8\log\left[\left(\frac{\varepsilon/D}{3.7}\right)^{1.11} + \frac{6.9}{Re}\right] \tag{10}$$

was used to approximate the friction factor, f, which was used to calculate the major losses in each possible line through the Darcy Weischbach equation,

$$\frac{\Delta p}{L} = f_D \cdot \frac{\rho}{2} \cdot \frac{\{v\}^2}{D} \tag{11}$$

With all of these in mind, the potential pressure drops (as normalized for a single meter's length) were tabulated, and from these it was determined that 0.18 inches, which reflects the nominal 1/4" VCR standards, was the ideal ID of the line. The model of the heater's walls was then modified to accommodate the lines, with three rows along three of the walls, and two on the wall which contains the VCR connectors. The geometry of this updated model was then used for validation inside the ANSYS Fluent Computational Fluid Dynamics (CFD) modeling process, which is discussed in the next chapter.

Chapter 4

CFD Analysis and Validation

Using this updated model, the heat flow was simulated using ANSYS Fluent, a computational fluid dynamics (CFD) focused submodule of the finite element analysis (FEA) suite of tools ANSYS offers. The goal of this analysis would be to verify the results of the mathematical analysis, mainly the conclusion that the cooling lines were sufficient for the amount of heat which would ever be applied in anticipated operating conditions. Additionally the work within ANSYS would need to correlate to the values determined by the mathematical analysis. Due to the nature of estimations, these were not expected to be exact matches, just values within a magnitude of the mathematical solution. Additionally, the solution offered by ANSYS was checked for internal consistency, as errors in the setup process could be identified through results which violate simple physical laws, such as continuity of matter.

The approximations and simplifications made here do not exactly match those made in the mathematical approach. One constraint limiting the scope of this analysis is that the version of ANSYS freely available to students limits the number of nodes, or elements, used in a given analysis. This limits the fidelity of the results based on the geometry analyzed. As such, superfluous geometry is excised to ensure the majority of elements are 'spent' on the specific volumes which needed to be analyzed. Because this analysis was focused on the efficacy of the water cooling lines, the only model analyzed was the walls which contained said lines. This raises the assumption that the heat held by the shutter and lid is negligible. For the lid this is a simple assumption, as it is held pressed against the walls such that conduction is maintained with the walls, and any heat it captured could easily flow to the walls. The heat retained by the shutter could be considerable, within the scope of this piece of equipment, however the containment of that heat is well accounted for; the wheel-based actuation solution means that very little of the cart could conduct heat to other components, and the radiative source of the heat is either focused upon the substrate or contained in full by an effectively insulating plate. With these considerations taken in mind,

the actual properties and techniques of the setup can be considered and discussed.

Because the method of design used CAD files designed inside of Autodesk Inventor, those CAD models were able to be imported directly into ANSYS, albeit converted from their proprietary file format to the more universal STEP format, which is the "Standard for the Exchange of Product model data", a file format for 3D objects defined by the International Organization for Standardization [8]. The file was opened within ANSYS's own geometry application, SpaceClaim, and then processed. SpaceClaim's utility in this step was that it could be used to verify the model's compatibility with ANSYS, label sections of faces and volumes which would be referenced later, and to identify the cavity occupied by the flowing water. This kind of problem is called a conjugate heat transfer problem, a problem dealing with the coupled bodies of a solid and a flowing fluid and their boundary in common [7]. ANSYS Fluent and computational FEA tools more generally are well equipped to solve these kinds of problems.

Having made all requisite preparations, the setup was provided the initial values and constants necessary to effectively solve the problem. Some of these were more simply determined than others. The fluid velocity at the inlet was set to 1 m/s and 300 K, per the water flow heat transfer calculations of section 3.2. At the outlet it was assumed that there was no gauge pressure, so that there was no backpressure or driving pressure considered. These assumptions all relied on the idea presented in section 3.2 that Lin Hall, the building this equipment will reside in, has a cooling water setup which far exceeds the needs of any system which could be designed for these purposes. The acceleration due to gravity was added to the parameters due to its ease of implementation and uncontroversial, if insignificant, effects. Finally, the radiative heat was accounted for. Because of the scope of its functionality, the heat flow boundary conditions for radiation was not used inside of ANSYS. The simplifications made to accommodate this analysis made that an inappropriate choice, and instead heat flux applied across the interior of the walls was used to represent the heat source. The amount of heat flux was determined as,

$$\text{Heat Flux } = \frac{\text{Heat}}{\text{Total Area}} \Rightarrow \frac{\text{Maximum Anticipated Heating Wattage}}{4 \cdot \text{Indivdual Interior Wall Area}} \tag{12}$$

and using the values below, one determined in section 3.1 and one taken from directly from the model,

$$\text{Maximum Anticipated Heating Wattage} = 600 \text{ W}$$

$$\text{Indivdual Interior Wall Area} = 8.941 \text{ in}^2 = 0.02307 \text{ m}^2$$

These values provide a heat flux of 26 kW/m^2. This is an inherently high estimation, as it assumes that at the highest anticipated power delivery the setup is also at steady-state, meaning it has been left on long enough that associated components have reached equilibrium temperatures, and finally it assumes that no heat is lost among the layers of tantalum foil insulation, whose sole purpose is to concentrate heat at the substrate and thus away from reaching the cooling walls.

Having assembled all prerequisites, including those correlated through or provided by prior work in this process, the most pressing questions can be answered. Firstly, what temperatures does the block reach?

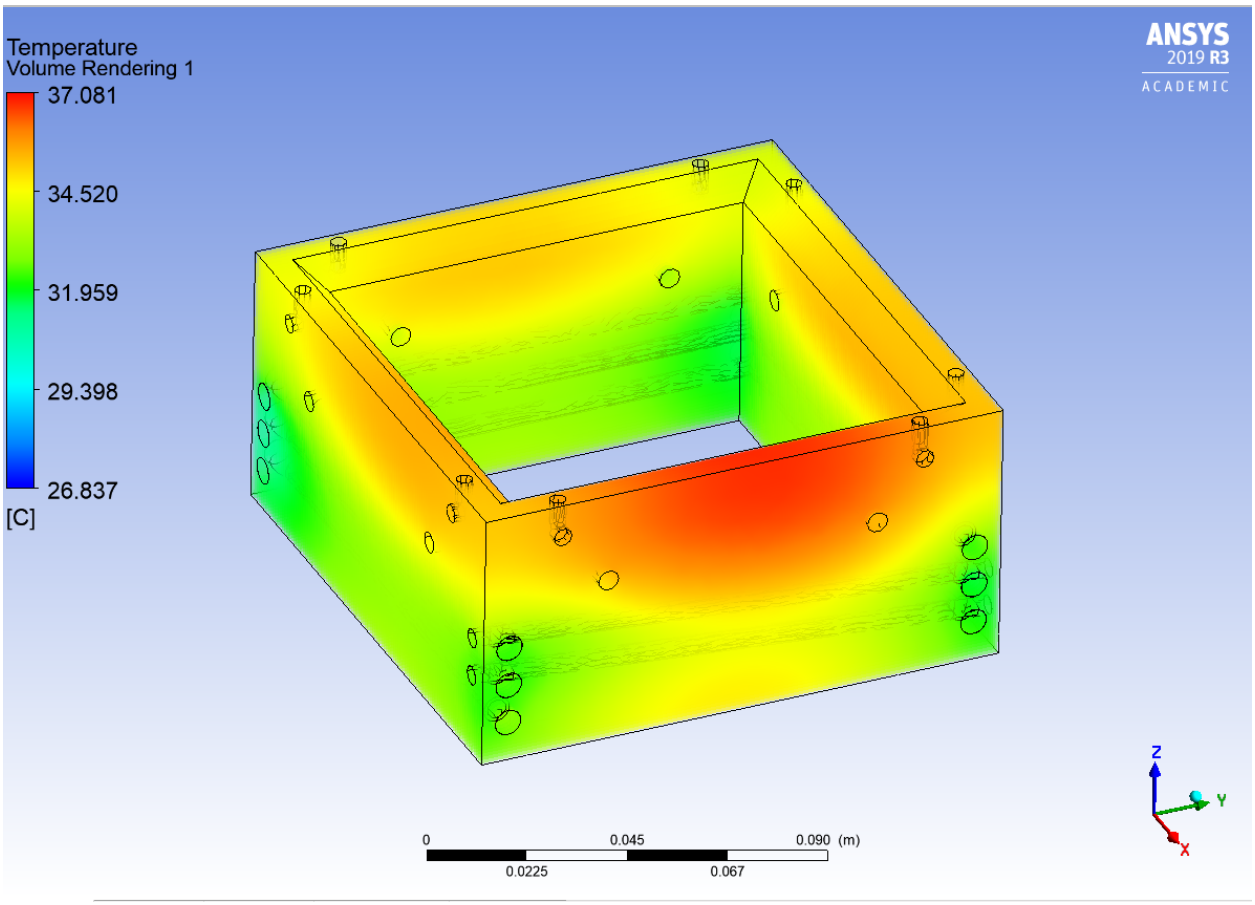

Figure 14: A volume rendering of the walls' temperature at a steady-state operating condition defined in the text.

Figure 14 shows the approximated distribution of temperature at steady-state. From the legend's upper bound one can see that the highest temperature seen within the copper block is 37 °C. The lower bound is not informative, as it's simply the temperature of the chilled water supply, which is among the predetermined boundary values. From this representation it's clear that the temperature should never get so great that the water lines struggle in the slightest. It's also clear from the model's heat distribution that the wall with two lines, rather than the three contained by the other walls, will be the hottest because of its lesser capacity for cooling. This is consistent with anticipated behavior, and thus increases confidence in the accuracy of this model. In addition, the walls are coolest where they're in contact with the cooling lines. The validity of this model, and its parameters, will be further reinforced later in this section.

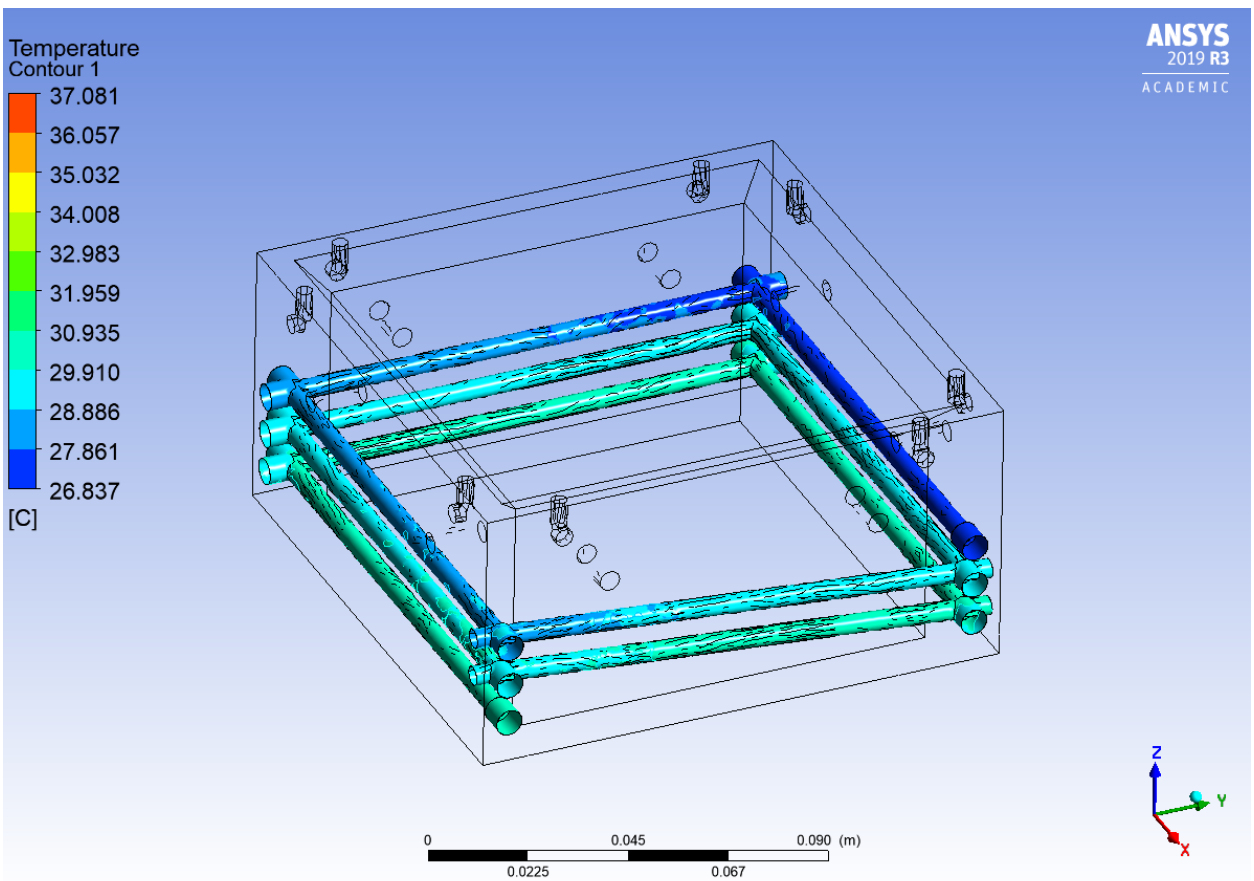

Figure 15: A rendering of the surface temperature within the cooling lines during operating conditions.

Figure 15 is also consistent with the behavior expected for the system. At the inlet it's at its

coolest, and as the water follows the perimeter of the walls it gradually heats up.

Being satisfied with the validity of the results so far, the final result to explore is the pressure at the outlet. The water flow calculations emphasized a turbulent flow, to maximize the efficacy of the water's heat transfer. This meant that the driving pressure of the system needed to be just enough to result in positive flow. In practice this may not make much of a difference, but for the purposes of exploring the theoretical capabilities of a system like this it's a more than useful exercise. Looking at the average pressure across the outlet and referencing ANSYS's legend reveals a negative pressure. Noting that this is a relative pressure, one can draw the conclusion that the water flow values have just overshot the initially calculated expectations. But, also noting the magnitude of the outlet pressure against the magnitude of the driving pressure, it's reasonable to assume this correlation between the mathematical approximation and the CFD approximation is indicative of a valid model.

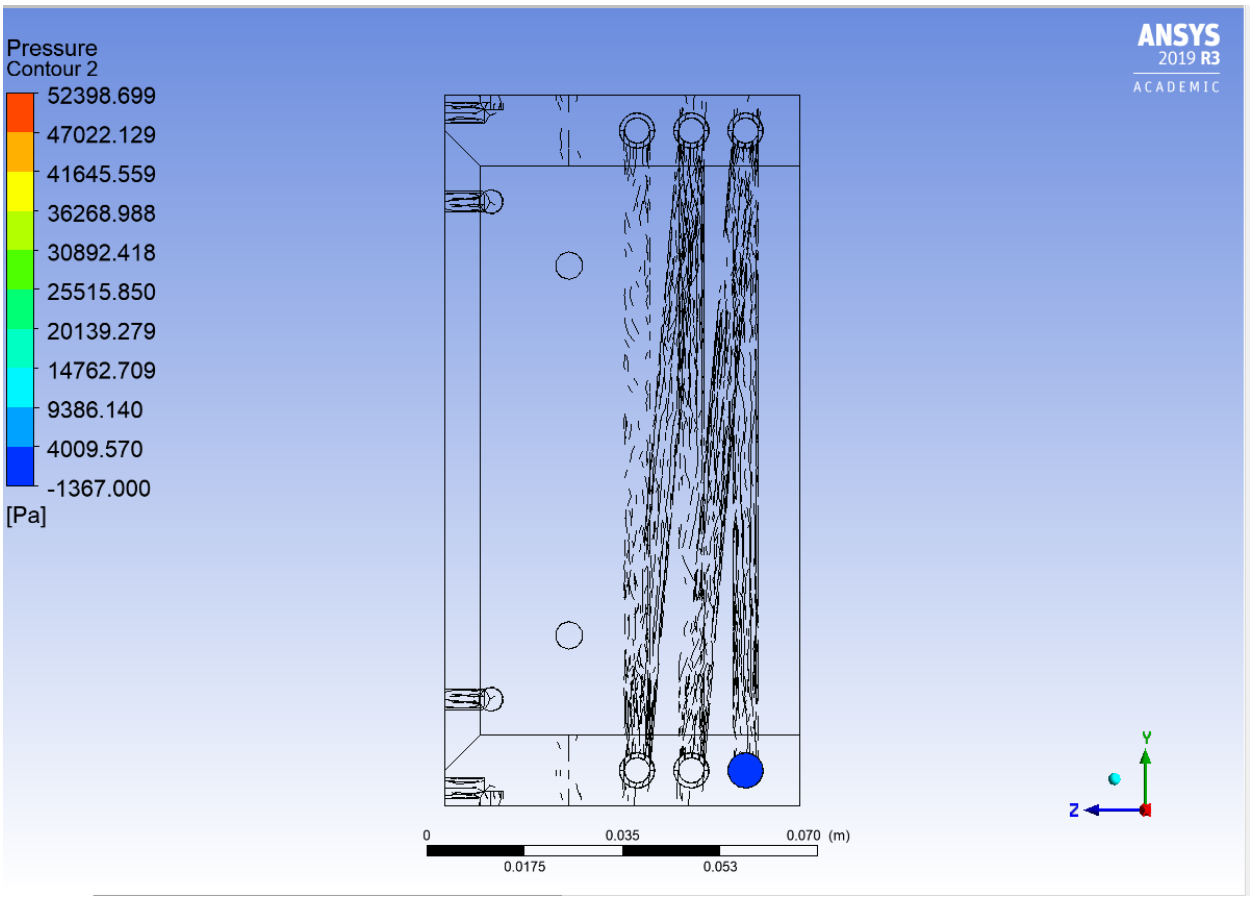

Figure 16: A rendering showing the simulated water pressure at the outlet while operating, notably approximating the average pressure across the entire outlet rather than delineating areas of high and low pressure.

Chapter 5

Use, Troubleshooting, and Future Application

5.1 Intended Use Procedure

The heater's design, and the provided procedure, is focused on use within our existing setup. However, the majority of procedures should be universal, or at least easily adapted, as vacuum chamber setups for PVD broadly operate on alike principals.

WHILE OPEN TO THE ATMOSPHERE

To access the substrate's mounting point, all a user will need to do is remove the lid from the assembly. This is more complicated than most lids, but still eminently doable. First, one needs to ensure the heat sink hardware has been properly secured. Briefly disconnecting it from its actuating assembly, where it's connected to a feedthrough, should be enough to do this. Next, one will need to free the lid by setting aside the lid tightening hardware. This can be accomplished by first removing the eight screws securing the four pieces of lid tightening hardware, and then the four pieces of hardware itself. A screwdriver can then be used to pry the lid off of the walls which it's resting on, using the slot designated for prying. Every effort should be made to lift the lid vertically, to keep the lid's stacked layers of tantalum foil from hitting those of the walls. Once the lid is clear from the rest of the assembly it can be inverted, revealing the alumina block where the substrate can be clipped into place. Following these steps in reverse order, one can reinstall the appropriate components and then prepare for the sealed procedures.

WHILE SEALED

Before the roughing pump is enabled, the user will need to ensure all components are in their appropriate places. The following checklist should generally be observed:

- The shutter-cart needs to be placed directly beneath the assembly.
- The heat-sink-block needs to be displaced so that it's not removing heat during the warming-

up process.

- The cooling lines should have water flowing through them.

These steps ensure not only that the alumina and substrate are efficiently heated, but that radiant heat isn't inadvertently released into the chamber, possibly damaging it.

Once the heater has reached a steady-state at its desired temperature, and the deposition sources are evaporating at a sufficient rate, the shutter-cart can be moved out from under the assembly and the thin film deposition can begin. Once the film has been deposited as desired, as monitored on a separate piece of equipment, the shutter-cart can be moved back in front of the sample, to prevent excess deposition, and the spring actuated heat-sink can be released onto the alumina block. This will accelerate the block's return to a more desirable temperature. Once that temperature has been reached, as assessed by a thermocouple, the chamber can be opened and the substrate can be removed.

To remove the substrate, the user will need to loosen the bolts retaining the lid, uncouple the cord which operates the spring-actuated heat-sink, and pull the lid upwards, utilizing the milled slot for a Phillips, or flat-head, screwdriver if the lid seems unduly stuck. Once removed one can easily access and remove the clips, and thus the substrate and deposited film, which retain the substrate to the alumina block, per Figure 9.

5.2 Troubleshooting

Because this design only exists on paper, it is impossible to now know all issues it may encounter in installation. However, the potential for some issues has been anticipated, with proposed solutions for those issues as well. Consideration needs to be given to the fact that this design focuses purely on the physical components, and does not delve into the specifics of the wiring needs, or other less tangible choices. This has been done in part for the sake of simplicity, but more broadly in light of the patent needs and implementation of such subsystems.

Of note is the potential for additional off-gassing as a result of frictional material removal ex-

posing new surface area for off gassing. Therefore, reducing frictional relationships is important to maintaining the chamber's integrity. The use of lubrication, which would provide a film of fluid to interface between any sliding bodies, is not possible here, as what constitute lubricants available at this scale of manufacture are all given to off-gassing, the very problem that needs mitigation. This problem guided many of the decisions made in this process, but certain compromises were made too. The cable which controls the position of the shutter-cart could incite this issue, as the static friction between it and the various pulleys it interfaces with may slip into kinetic friction and cause this issue. That is why the cables need to be held taut, to reduce the possibility of this occurrence. Additionally, should tightening these cables fail to solve the issue, there is an additional provided design for an actuation solution with phalanges-like rods rotating through bearings as revolute joints. Additional sources of frictional removed material might be the tight fit between the top of the shutter-cart and the bottom of the top heater. Possible interference here would be solved through additional machining to reach the desired fit, or preferably adjusting the vertical position of the shutter-cart and rails through their mounting points on the heater support.

Additionally, and far more obviously, nixing the custom actuary components in favor of commercial options, and swapping in a linear feedthrough is a simple solution, albeit one with a price-tag several hundred-times the materials budget for the designs provided herein which rely on currently owned rotary feedthroughs.

Should the cart prove difficult to actuate with the initial cable setup, there are provided alternative pulley sizes, to accommodate reducing, or increasing, the number of rotations required to move the shutter-cart. If this fails to solve the problem, once again, there is the potential to instead use a linear feedthrough to actuate the cart.

5.3 Future Applications

This setup will be used for thin-film depositions for the foreseeable future, and some of the accommodations this could require have already been accounted for. For example, the significant

heating requirements of a process like gold deposition, and deposition onto gold, were used as an upper bound during the design process. Beyond this, the assembly is compartmentalized such that many of the components can be replaced with correlating alternative parts.

Chapter 6

Conclusion

Providing an evenly heated substrate is key to achieving a desirable thin film for STM applications. Achieving this evenness has been accomplished in different ways, to different degrees of success, in setups like this one in many previous labs. By integrating two heaters, designing with insulation in mind, and closely integrating water-cooling, the overall complexity of the design was greatly increased, but with that increase came a greater guarantee of having brought the substrate a well developed, even temperature. This holds the potential for producing films within the lab of much greater quality than could be manufactured previously, or potentially better than films for purchase.

By designing around making the substrate as accessible as possible, as well as integrating a solution to quickly remove heat from the setup, the design focuses specifically on the workflow required by thin film manufacture. Since this chamber will be dedicated to that process, the ability to prioritize the end-user's needs and consumed time over the universalized features of commercial heaters will hopefully be a boon to the system's overall efficiency and use.

Of note is the inability, due to the limitations of time, to begin physical manufacture of parts within the design. While this was disappointing, it meant that work further than merely what would have been built could be completed, and that tools were able to be excised to better guarantee a success when the parts are eventually made and assembled. While ordinarily some pieces of this design would have been adjusted through trial and error in the physical world, here it was necessary to check, and double-check, results which would otherwise might have merely been assumed. This ended up being a revealing part of the overall design process, as givens such as the effectiveness of tantalum sheets for insulation, or the effectiveness of the water lines embedded in the copper walls, were analyzed, and proven to be true, rather than simply taken for granted.

Chapter 7

Acknowledgments

Firstly I would like to thank the Bumm research group for providing the means and platform for my research, and particularly Dr. Bumm for his guidance and mentorship in this process. I am also grateful for the School of Aerospace and Mechanical Engineering for accommodating my work within it, and Dr. Liu for allowing me to pursue this project as I desired.

I would also like to thank Alexandra Elbakyan for her continued work to keep knowledge freely accessible through Sci-Hub, as well as the work of the Wikimedia Foundation and its stewardship of Wikipedia.

Chapter 8

Drawings

PDFs of Inventor

Drawings Appended

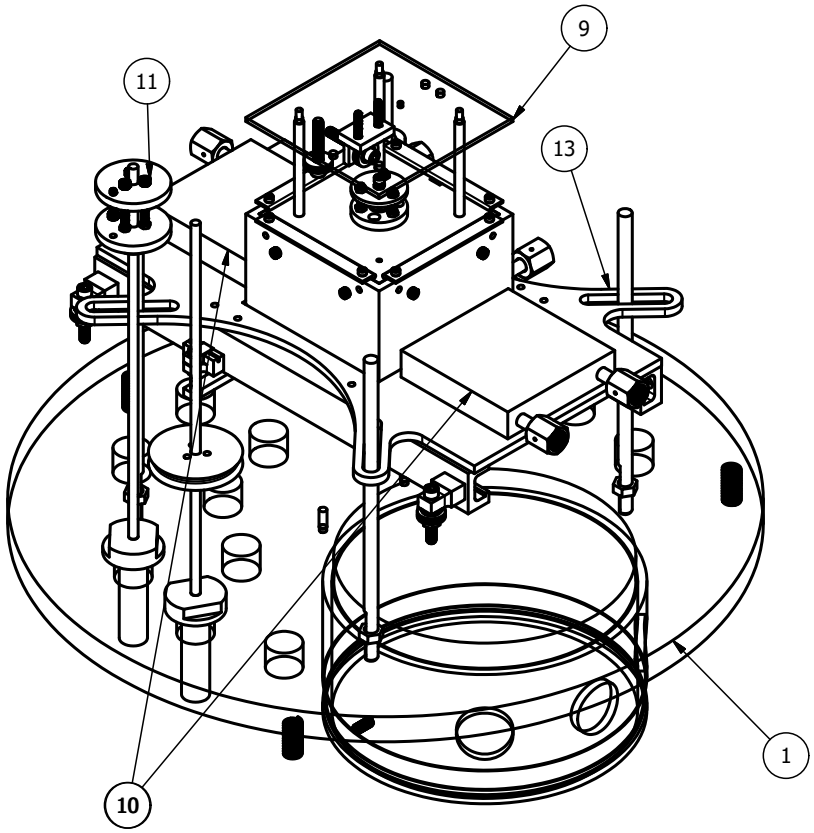

PARTS LIST		
ITEM	QTY	PART NUMBER
1	1	Base Well
9	1	heater holder assembly
10	2	Side shutter Cooling Shield
11	1	Spool redux
12	1	NuBottomCart
13	1	ExtraneousSupportMaterial

GALLOGLY COLLEGE OF ENGINEERING
SCHOOL OF AEROSPACE AND MECHANICAL ENGINEERING
The UNIVERSITY of OKLAHOMA

Drawn by Bryan Boone

Project Name	Material		Date	Revision	Sheet
Allara Thermal Evaporator, Lin Hall 120	Full Chamber		7/24/2020	1	1 of 1
Part Name	**Quantity**	**Scale**	**Point of Contact**		
Full Chamber	1	0.12:1	L.A. Bumm 405-364-7253, OU/Physics		
File Name					
C:\Users\bmboo\Documents\Inventor\HeatEvaporator\Updated Chamber Setup.iam					

PARTS LIST		
ITEM	QTY	PART NUMBER
1	1	Copper Walls
2	1	Copper Top
5	8	8-32 0.328 Lg Helical Coil8-32 328 mil 96246A144_HELICAL INSERT
6	8	6-32 0.276 Lg Helicoil6-32 276 mil 96246A102_HELICAL INSERT
9	8	8-32 bolt 0.75 length 90843A180_ CLEANED-AND-BAGGED 18-8 SOCKET HEAD SCREW
11	8	8-32 thin nut 90730A009_TYPE 18-8 STAINLESS STEEL NARROW HEX NUT
13	8	6-32 vented bolt 93235A144_VENTED 18-8 SS SOCKET HEAD CAP SCREW
14	4	Clamp for Coppper Top 2
15	2	pseudo VCR fitting butt long 9066N180_ULTRA-HIGH-POLISH BUTT-WELD FITTING
16	2	pseudo VCR fitting female nut 9066N250_ULTRA-HIGH-POLISH BUTT-WELD FITTING
17	1	spring sink setup 2
18	1	lifting subassembly
19	1	Plate Pulley Mount with Standoffs

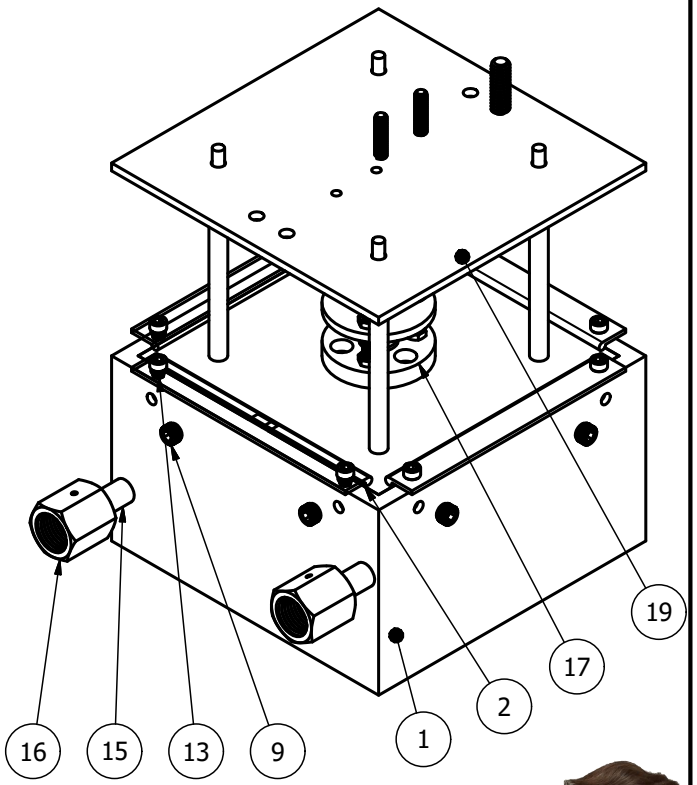

GALLOGLY COLLEGE OF ENGINEERING
SCHOOL OF AEROSPACE AND MECHANICAL ENGINEERING
The UNIVERSITY of OKLAHOMA

Drawn by Bryan Boone

Project Name Allara Thermal Evaporator, Lin Hall 120	*Material* Mixed		*Date* 7/28/2020	*Revision* 1	*Sheet* 1 of 5
Part Name Top Heater in Full	*Quantity* 1	*Scale* 1:2	*Point of Contact* **L.A. Bumm 405-364-7253, OU/Physics**	
File Name C:\Users\bmboo\Documents\Inventor\HeatEvaporator\heater\heater holder assembly.iam				

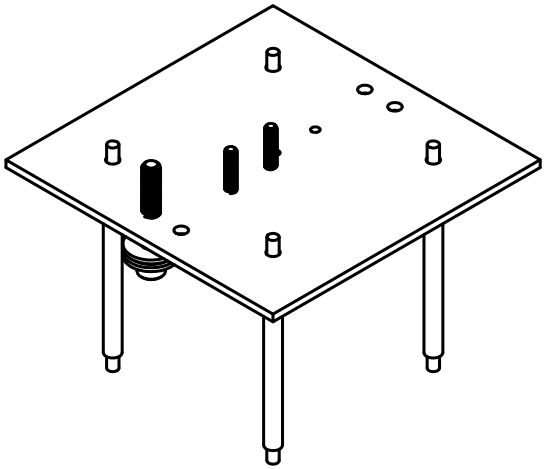

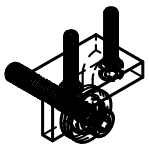

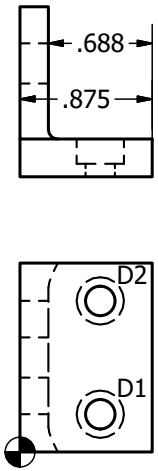

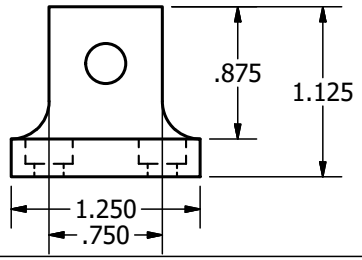

HOLE TABLE			
HOLE	XDIM	YDIM	DESCRIPTION
D1	.53	.25	Ø.194 THRU ⌴ Ø.313 ↧ .164
D2	.53	1.00	

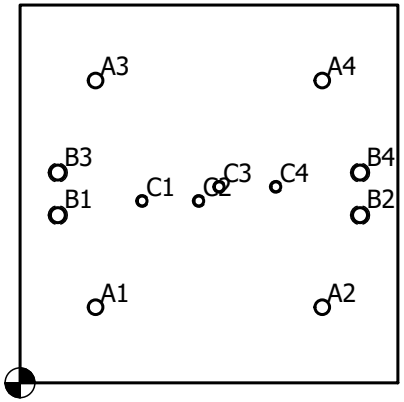

HOLE TABLE			
HOLE	XDIM	YDIM	DESCRIPTION
A1	1.00	1.00	Ø.194 THRU
A2	4.00	1.00	
A3	1.00	4.00	
A4	4.00	4.00	
B1	.50	2.22	1/4-20 UNC - 2B
B2	4.50	2.22	
B3	.50	2.78	
B4	4.50	2.78	
C1	1.61	2.41	8-32 UNC - 2B
C2	2.36	2.41	
C3	2.64	2.59	
C4	3.39	2.59	

GALLOGLY COLLEGE OF ENGINEERING
SCHOOL OF AEROSPACE AND MECHANICAL ENGINEERING
The UNIVERSITY of OKLAHOMA

Drawn by Bryan Boone

Project Name	Material	Date	Revision	Sheet
Allara Thermal Evaporator, Lin Hall 120	Steel	7/28/2020	1	2 of 5

Part Name	Quantity	Scale	Point of Contact
Topmost Plate for Pulleys	1	1:2	L.A. Bumm 405-364-7253, OU/Physics

File Name: C:\Users\bmboo\Documents\Inventor\HeatEvaporator\heater\Plate Pulley Mount with Standoffs.iam

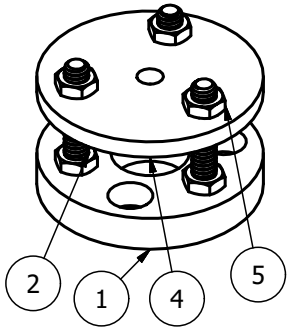

PARTS LIST		
ITEM	QTY	PART NUMBER
1	1	bottom plate v2
2	3	92196A198_18-8 STAINLESS STEEL SOCKET HEAD CAP SCREW
4	1	top plate v2
5	3	8-32 thin nut 90730A009_TYPE 18-8 STAINLESS STEEL NARROW HEX NUT

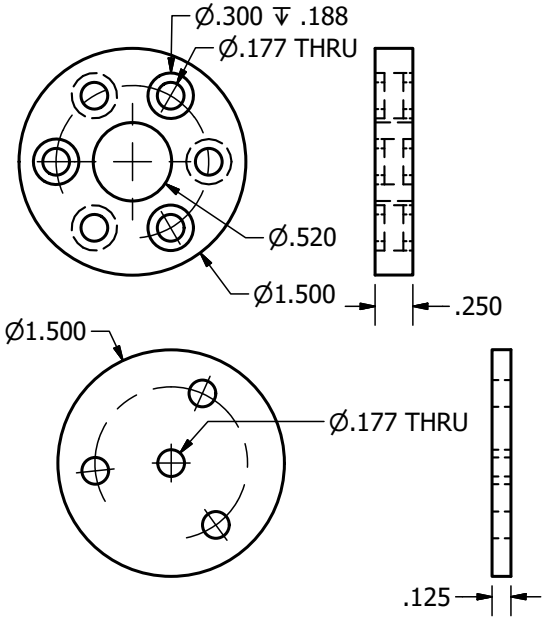

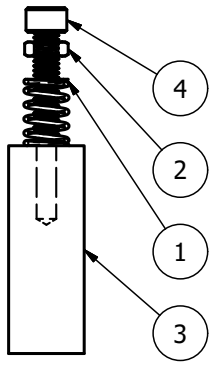

PARTS LIST		
ITEM	QTY	PART NUMBER
1	1	spring 440lg 300od 236id 9657K247_COMPRESSION SPRING
2	1	8-32 thin nut 90730A009_TYPE 18-8 STAINLESS STEEL NARROW HEX NUT
3	1	heat sink v2
4	1	no8 1 in vented 90841A230_ CLEANED-AND-BAGGED VENTED SOCKET HEAD SCREW

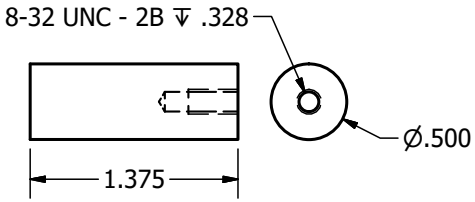

GALLOGLY COLLEGE OF ENGINEERING
SCHOOL OF AEROSPACE AND MECHANICAL ENGINEERING
The UNIVERSITY of OKLAHOMA

Drawn by Bryan Boone

Project Name	Material		Date	Revision	Sheet
Allara Thermal Evaporator, Lin Hall 120	Steel		7/28/2020	1	3 of 5
Part Name	**Quantity**	**Scale**	**Point of Contact**		
Spring-loaded Heatsink	1	1:1	L.A. Bumm 405-364-7253, OU/Physics		
File Name C:\Users\bmboo\Documents\Inventor\HeatEvaporator\heater\spring sink setup\lifting subassembly.iam					

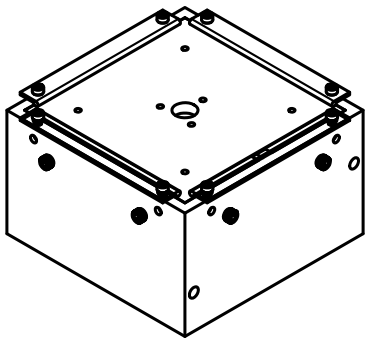

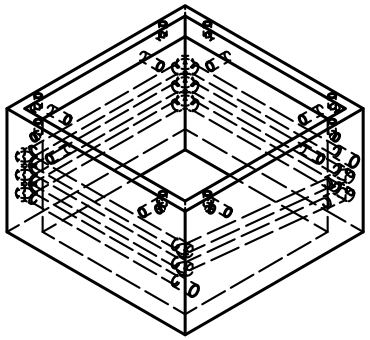

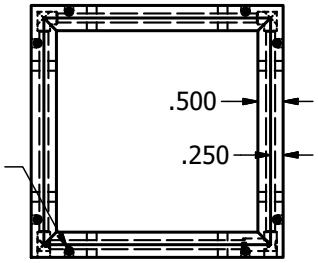

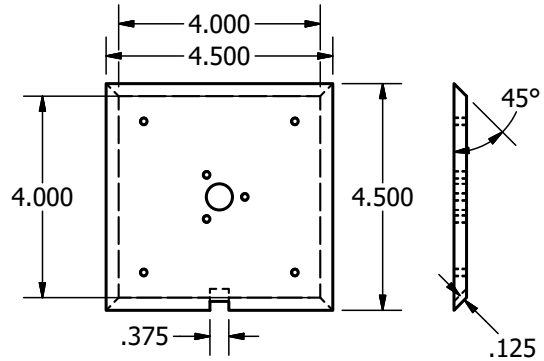

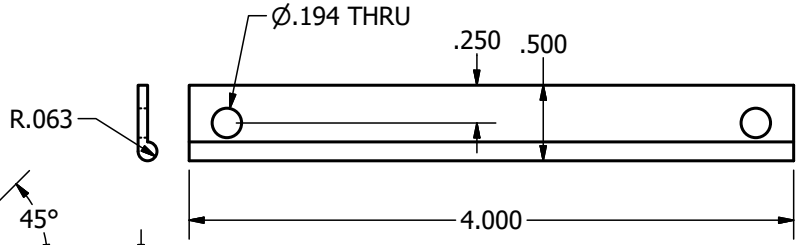

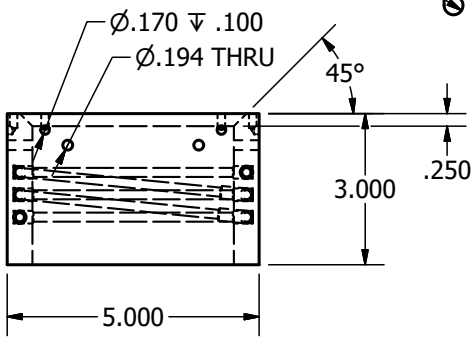

GALLOGLY COLLEGE OF ENGINEERING
SCHOOL OF AEROSPACE AND MECHANICAL ENGINEERING
The UNIVERSITY of OKLAHOMA

Drawn by Bryan Boone

Project Name	Material		Date	Revision	Sheet
Allara Thermal Evaporator, Lin Hall 120	Copper and Steel		7/28/2020	1	4 of 5
Part Name	**Quantity**	**Scale**	**Point of Contact**		
Lid, Top walls, and retaining clamps	1 and 4	1:3 and 1:1	L.A. Bumm 405-364-7253, OU/Physics		
File Name	C:\Users\bmboo\Documents\Inventor\HeatEvaporator\heater\heater holder assembly.iam				

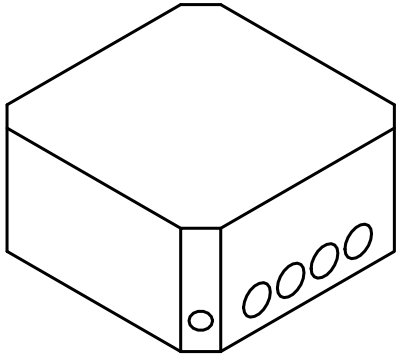

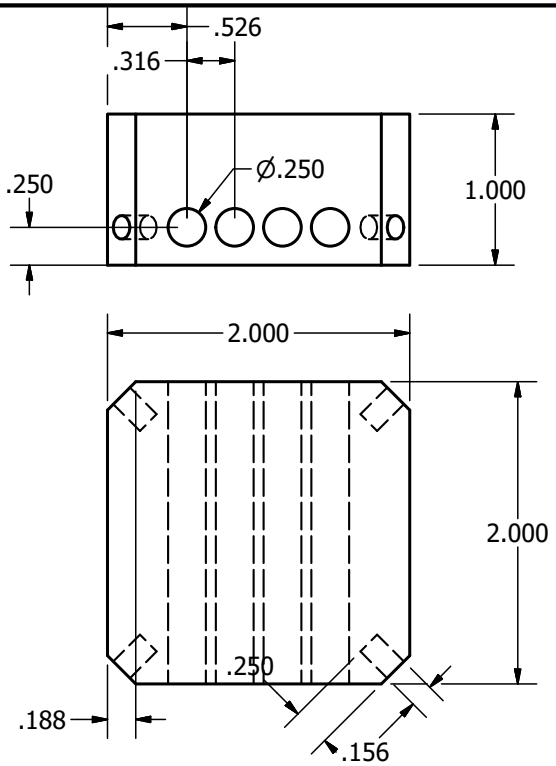

GALLOGLY COLLEGE OF ENGINEERING
SCHOOL OF AEROSPACE AND MECHANICAL ENGINEERING
The UNIVERSITY of OKLAHOMA

Drawn by Bryan Boone

Project Name	Material		Date	Revision	Sheet
Allara Thermal Evaporator, Lin Hall 120	Alumina		7/28/2020	1	5 of 5
Part Name	**Quantity**	**Scale**	**Point of Contact**		
Alumina Heater	1	1:1	L.A. Bumm 405-364-7253, OU/Physics		
File Name C:\Users\bmboo\Documents\Inventor\HeatEvaporator\heater\draftAluminaBlock.ipt					

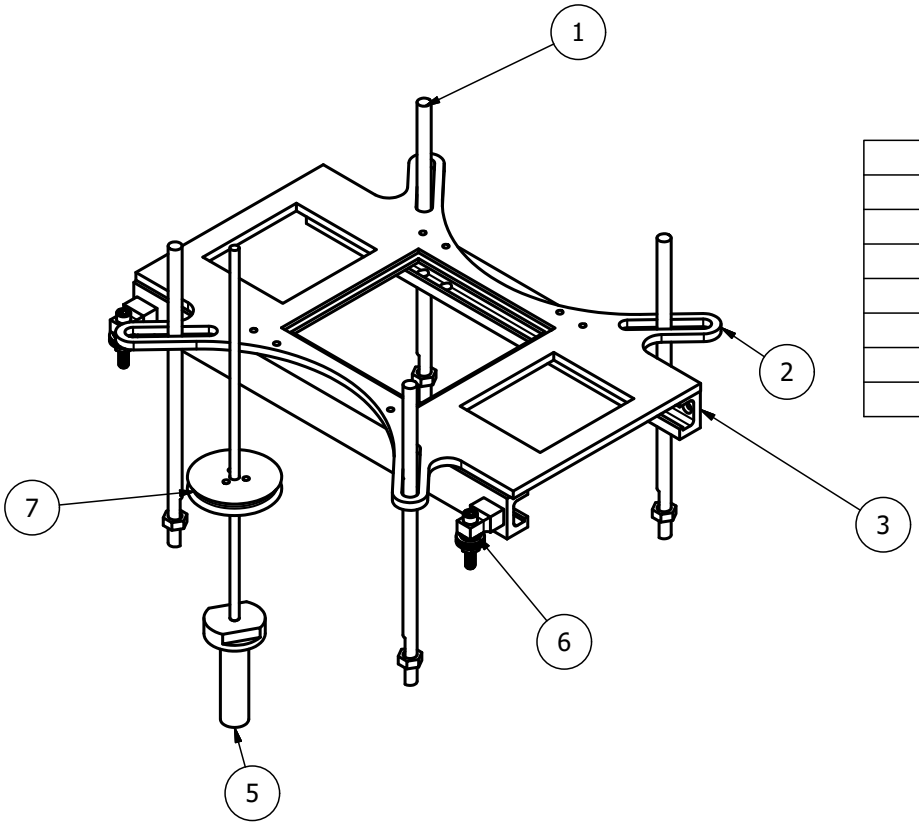

PARTS LIST		
ITEM	QTY	PART NUMBER
1	4	heater structure rod
2	1	heater support rev 2
3	2	bottom rail 3
5	1	linearRailAssembly
6	2	rail base
7	1	base

GALLOGLY COLLEGE OF ENGINEERING
SCHOOL OF AEROSPACE AND MECHANICAL ENGINEERING
The UNIVERSITY of OKLAHOMA

Drawn by Bryan Boone

Project Name	Material		Date	Revision	Sheet
Allara Thermal Evaporator, Lin Hall 120	Steel		7/28/2020	1	1 of 5
Part Name	**Quantity**	**Scale**	**Point of Contact**		
Infrastructure parts	1	1:3	L.A. Bumm 405-364-7253, OU/Physics		
File Name C:\Users\bmboo\Documents\Inventor\HeatEvaporator\Drawings\ExtraneousSupportMaterial.iam					

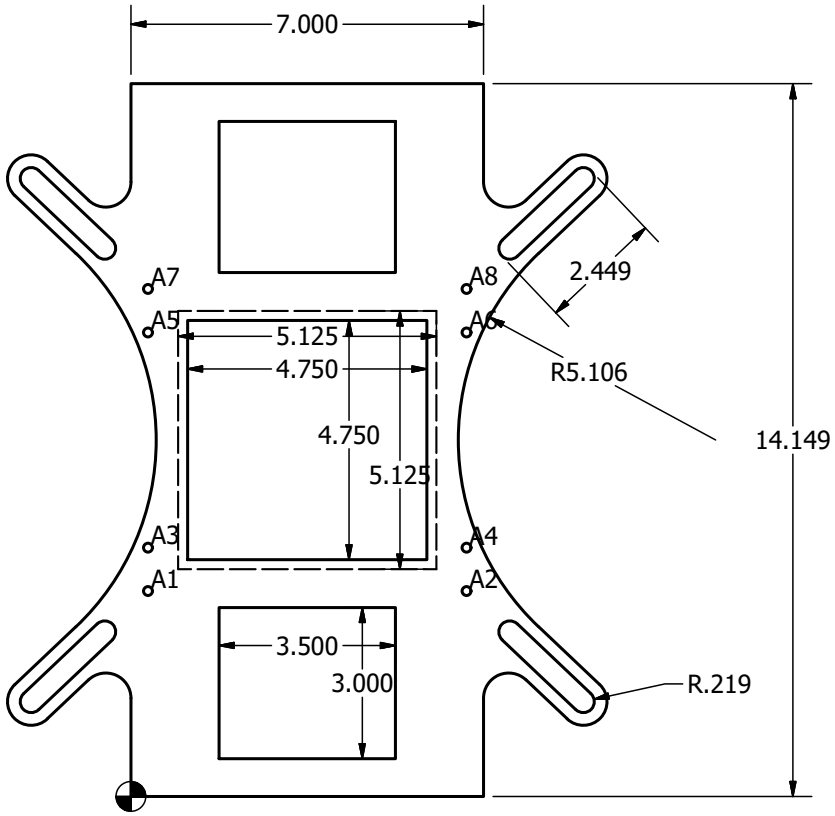

HOLE TABLE			
HOLE	XDIM	YDIM	DESCRIPTION
A1	.34	4.08	Ø.177 THRU
A2	6.66	4.08	
A3	.34	4.94	
A4	6.66	4.94	
A5	.34	9.21	
A6	6.66	9.21	
A7	.34	10.07	
A8	6.66	10.07	

GALLOGLY COLLEGE OF ENGINEERING
SCHOOL OF AEROSPACE AND MECHANICAL ENGINEERING
The UNIVERSITY of OKLAHOMA

Drawn by Bryan Boone

Project Name	Material		Date	Revision	Sheet
Allara Thermal Evaporator, Lin Hall 120	Steel		7/28/2020	1	2 of 5
Part Name	**Quantity**	**Scale**	**Point of Contact**		
Frame	1	1:3	L.A. Bumm 405-364-7253, OU/Physics		
File Name C:\Users\bmboo\Documents\Inventor\HeatEvaporator\heater\heater support rev 2.ipt					

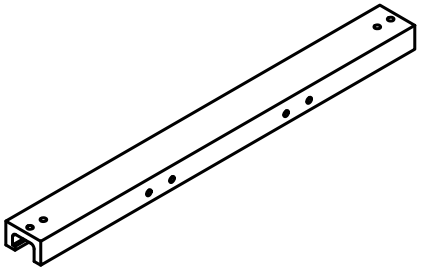

HOLE TABLE			
HOLE	XDIM	YDIM	DESCRIPTION
A1	.25	.65	Ø.177 THRU Ø.332 X 82°
A2	.75	.65	
A3	13.25	.65	
A4	13.75	.65	

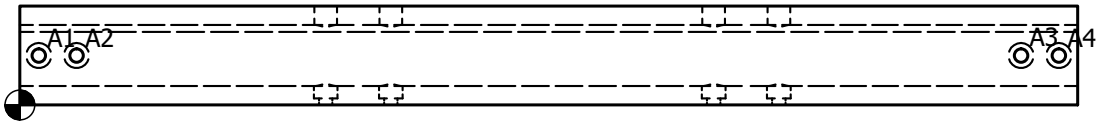

HOLE TABLE			
HOLE	XDIM	YDIM	DESCRIPTION
A1	4.05	.32	Ø.300 ↧ 1.059
A2	4.91	.32	
A3	9.18	.32	
A4	10.04	.32	
B1	4.05	.32	Ø.177 THRU ⌴ Ø.313 ↧ .164
B2	4.91	.32	
B3	9.18	.32	
B4	10.04	.32	

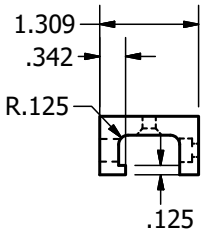

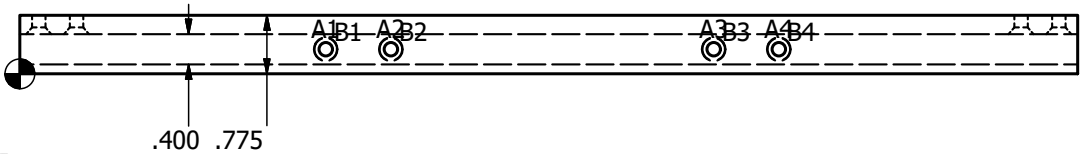

GALLOGLY COLLEGE OF ENGINEERING
SCHOOL OF AEROSPACE AND MECHANICAL ENGINEERING
The UNIVERSITY of OKLAHOMA

Drawn by Bryan Boone

Project Name	Material		Date	Revision	Sheet
Allara Thermal Evaporator, Lin Hall 120	Steel		7/28/2020	1	3 of 5
Part Name	**Quantity**	**Scale**	**Point of Contact**		
Rail	2	1:4 and 1:2	L.A. Bumm 405-364-7253, OU/Physics		
File Name C:\Users\bmboo\Documents\Inventor\HeatEvaporator\heater\bottom rail 3.ipt					

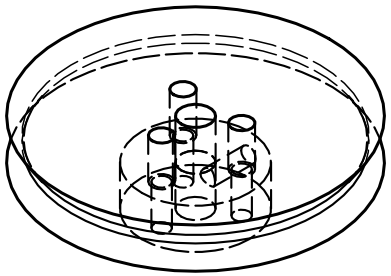

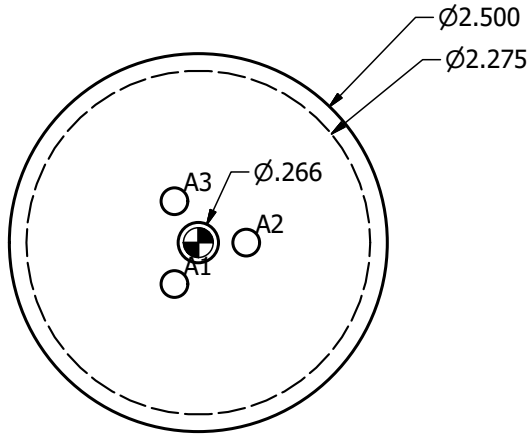

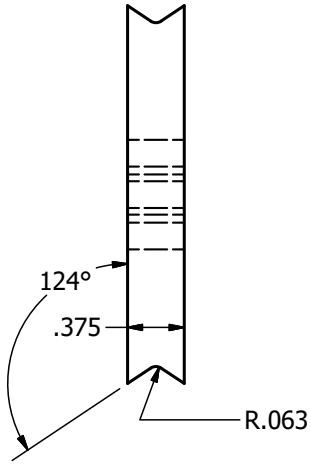

HOLE TABLE			
HOLE	XDIM	YDIM	DESCRIPTION
A1	-.16	-.27	Ø.177 ↧ 1.000
A2	.32	.00	
A3	-.16	.27	

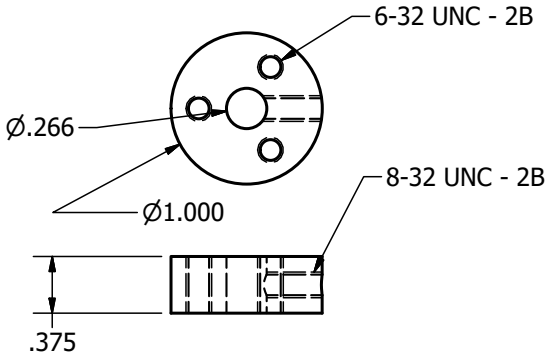

GALLOGLY COLLEGE OF ENGINEERING
SCHOOL OF AEROSPACE AND MECHANICAL ENGINEERING
The UNIVERSITY of OKLAHOMA

Drawn by Bryan Boone

Project Name	Material		Date	Revision	Sheet
Allara Thermal Evaporator, Lin Hall 120	Steel		7/28/2020	1	4 of 5
Part Name	**Quantity**	**Scale**	**Point of Contact**		
Base Pulley	1	1:1	L.A. Bumm 405-364-7253, OU/Physics		
File Name C:\Users\bmboo\Documents\Inventor\HeatEvaporator\heater\cable driven cart actuation\base.iam					

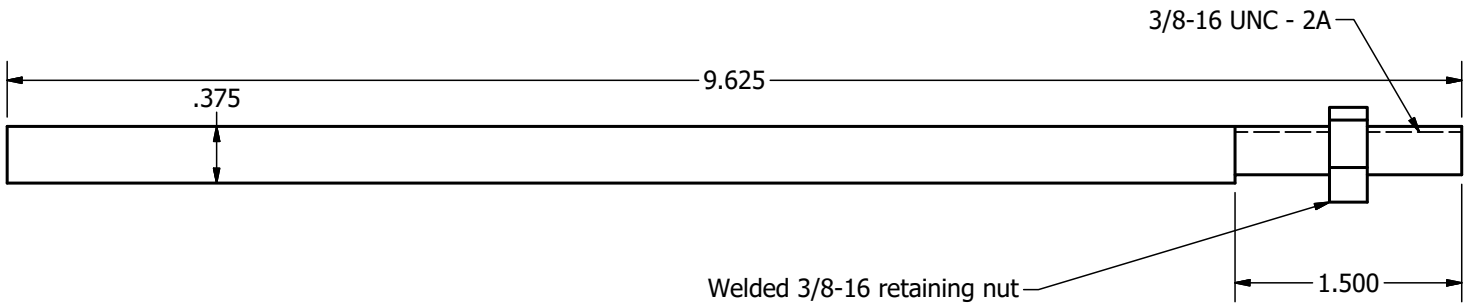

GALLOGLY COLLEGE OF ENGINEERING
SCHOOL OF AEROSPACE AND MECHANICAL ENGINEERING
The UNIVERSITY of OKLAHOMA

Drawn by Bryan Boone

Project Name	Material		Date	Revision	Sheet
Allara Thermal Evaporator, Lin Hall 120	Steel		7/28/2020	1	5 of 5
Part Name	**Quantity**	**Scale**	**Point of Contact**		
Threaded Support Rod	4	1:1	L.A. Bumm 405-364-7253, OU/Physics		
File Name	C:\Users\bmboo\Documents\Inventor\HeatEvaporator\heater\heater structure rod.ipt				

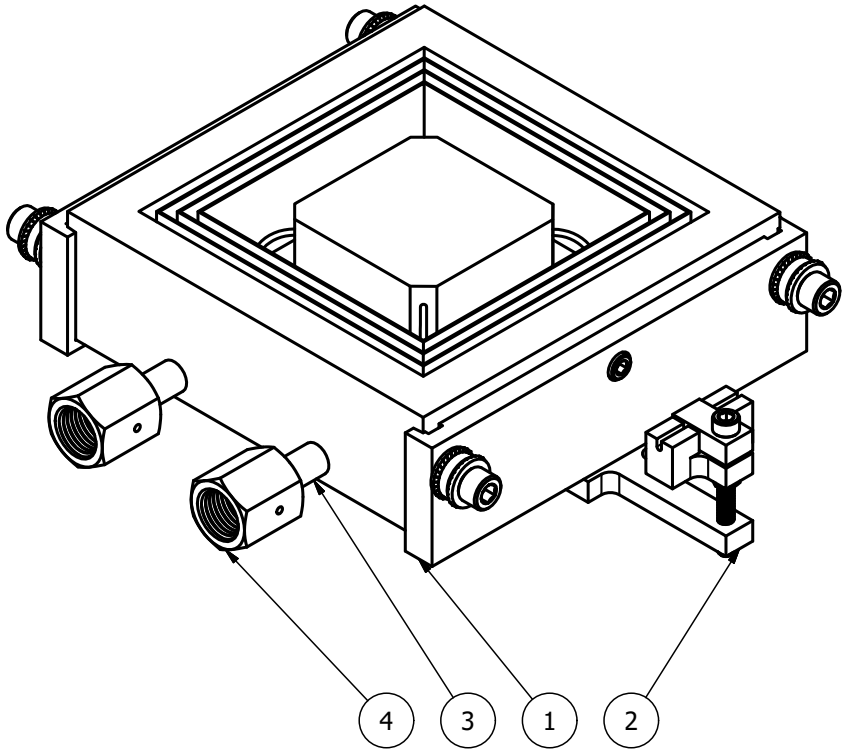

PARTS LIST		
ITEM	QTY	PART NUMBER
1	1	Bottom Heater Assembly
2	1	assembled v2 cord capture
3	2	pseudo VCR fitting butt long 9066N180_ULTRA-HIGH-POLISH BUTT-WELD FITTING
4	2	pseudo VCR fitting female nut 9066N250_ULTRA-HIGH-POLISH BUTT-WELD FITTING

GALLOGLY COLLEGE OF ENGINEERING
SCHOOL OF AEROSPACE AND MECHANICAL ENGINEERING
The UNIVERSITY of OKLAHOMA

Drawn by Bryan Boone

Project Name Allara Thermal Evaporator, Lin Hall 120	*Material* Mixed		*Date* 7/28/2020	*Revision* 1	*Sheet* 1 of 4
Part Name Shutter-Cart	*Quantity* 1	*Scale* 2:3	*Point of Contact* **L.A. Bumm 405-364-7253, OU/Physics**	
File Name C:\Users\bmboo\Documents\Inventor\HeatEvaporator\Drawings\NuBottomCart.iam				

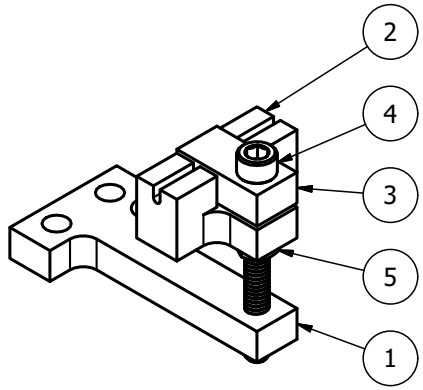

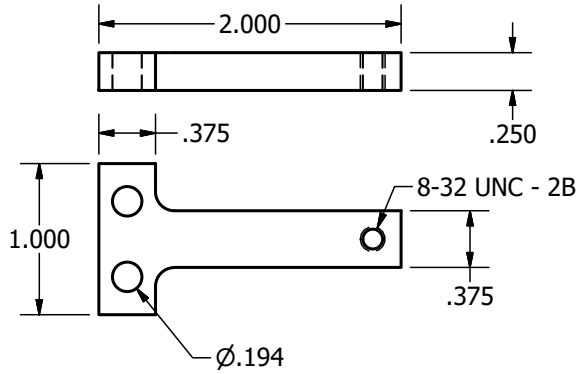

PARTS LIST		
ITEM	QTY	PART NUMBER
1	1	base
2	1	bottom clamp
3	1	top clamp
4	1	no8-32 1 1-2lg 92196A178_18-8 STAINLESS STEEL SOCKET HEAD CAP SCREW
5	1	8-32 thin nut 90730A009_TYPE 18-8 STAINLESS STEEL NARROW HEX NUT_MIR

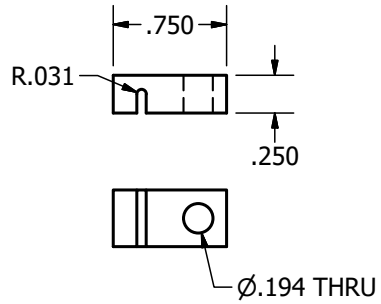

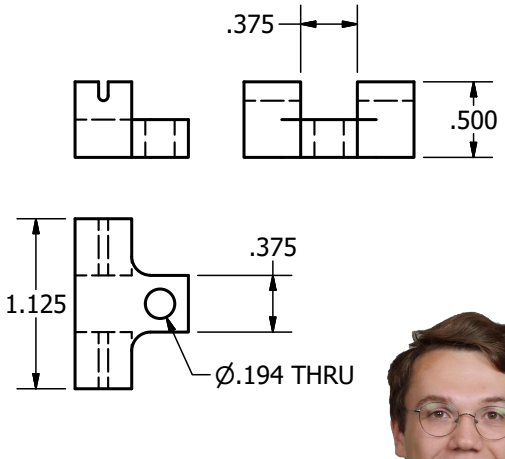

GALLOGLY COLLEGE OF ENGINEERING
SCHOOL OF AEROSPACE AND MECHANICAL ENGINEERING
The UNIVERSITY of OKLAHOMA

Drawn by Bryan Boone

Project Name Allara Thermal Evaporator, Lin Hall 120	*Material* Steel		*Date* 7/28/2020	*Revision* 1	*Sheet* 2 of 4
Part Name Cord Capture	*Quantity* 1	*Scale* 1:1	*Point of Contact* **L.A. Bumm 405-364-7253, OU/Physics**	
File Name C:\Users\bmboo\Documents\Inventor\HeatEvaporator\heater\cord capture\v2\assembled v2 cord capture.iam				

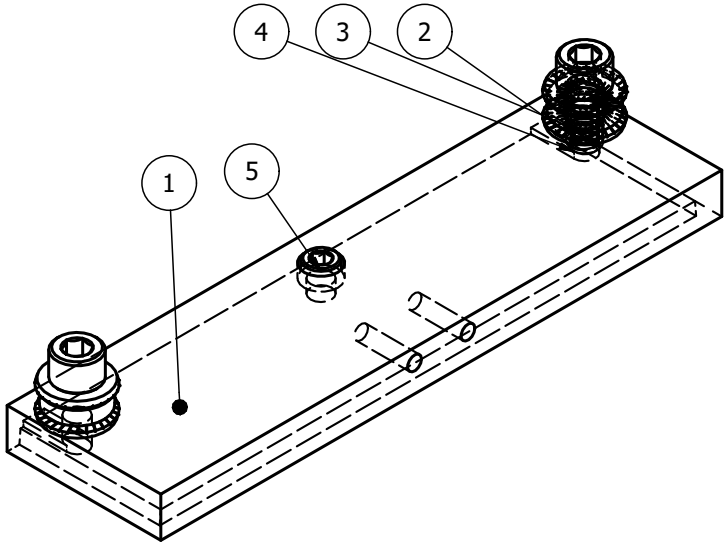

PARTS LIST		
ITEM	QTY	PART NUMBER
1	1	carriage 2
2	4	1-4 in conical lock washer 90127A029_STEEL BELLEVILLE SPRING LOCK WASHER
3	2	bearings from mdc vacuum
4	2	1-4 IN 20 SCREW 1-2 LG 92196A537_18-8 STAINLESS STEEL SOCKET HEAD CAP SCREW
5	2	no 8 half inch socket head screw 92196A194_18-8 STAINLESS STEEL SOCKET HEAD CAP SCREW

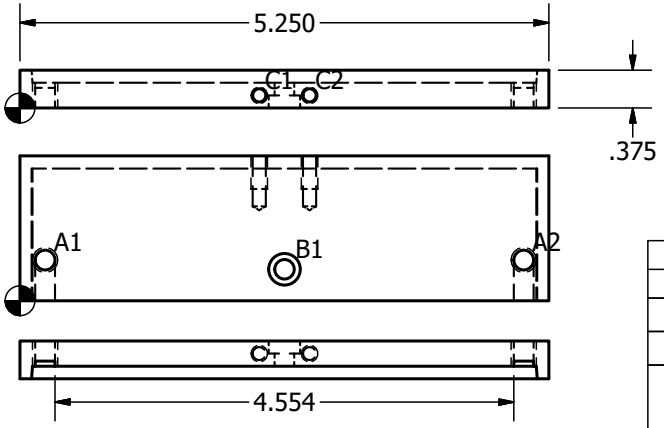

HOLE TABLE			
HOLE	XDIM	YDIM	DESCRIPTION
C1	2.38	.13	8-32 UNC - 2B ↧ .328
C2	2.88	.13	

HOLE TABLE			
HOLE	XDIM	YDIM	DESCRIPTION
A1	.25	.40	1/4-20 UNC - 2B
A2	5.00	.40	
B1	2.63	.31	∅.194 THRU ⌴ ∅.313 ↧ .125

GALLOGLY COLLEGE OF ENGINEERING
SCHOOL OF AEROSPACE AND MECHANICAL ENGINEERING
The UNIVERSITY of OKLAHOMA

Drawn by Bryan Boone

Project Name	Material	Date	Revision	Sheet
Allara Thermal Evaporator, Lin Hall 120	Steel	7/28/2020	1	3 of 4

Part Name	Quantity	Scale	Point of Contact
Cart Half	2	1:1 and 2:3	L.A. Bumm 405-364-7253, OU/Physics

File Name: C:\Users\bmboo\Documents\Inventor\HeatEvaporator\heater\bottom carriage 2.iam

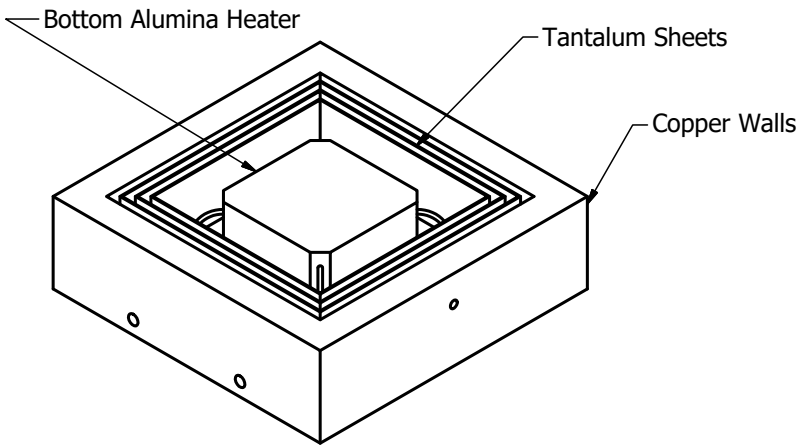

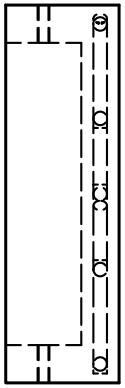

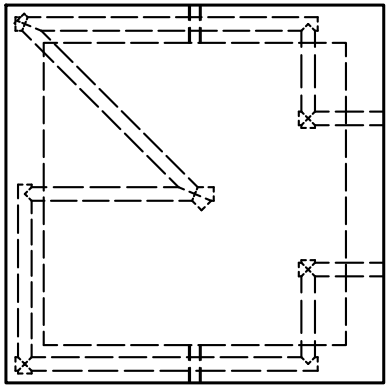

GALLOGLY COLLEGE OF ENGINEERING
SCHOOL OF AEROSPACE AND MECHANICAL ENGINEERING
The UNIVERSITY of OKLAHOMA

Drawn by Bryan Boone

Project Name Allara Thermal Evaporator, Lin Hall 120	*Material* Copper, Tantalum		*Date* 7/28/2020	*Revision* 1 / *Sheet* 4 of 4
Part Name Bottom Heater	*Quantity* 1	*Scale* 1:2	*Point of Contact* **L.A. Bumm 405-364-7253, OU/Physics**	
File Name C:\Users\bmboo\Documents\Inventor\HeatEvaporator\heater\Bottom Heater Assembly.iam				

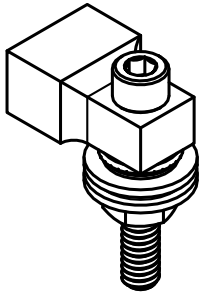

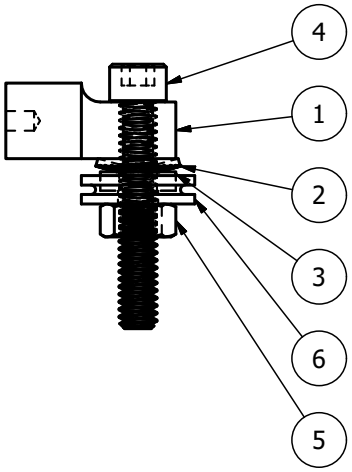

PARTS LIST		
ITEM	QTY	PART NUMBER
1	1	rail mount for pulleys
2	1	90127A029_STEEL BELLEVILLE SPRING LOCK WASHER
3	1	bearings from mdc vacuum
4	1	1-4 20 screw 1 1-2 long 92196A706_18-8 STAINLESS STEEL SOCKET HEAD CAP SCREW
5	1	91845A029_TYPE 18-8 STAINLESS STEEL HEX NUT
6	1	pulley default shape

GALLOGLY COLLEGE OF ENGINEERING
SCHOOL OF AEROSPACE AND MECHANICAL ENGINEERING
The UNIVERSITY of OKLAHOMA

Drawn by Bryan Boone

Project Name Allara Thermal Evaporator, Lin Hall 120	*Material* Steel		*Date* 7/28/2020	*Revision* 1	*Sheet* 1 of 2
Part Name Rail Pulley Mount	*Quantity* 2	*Scale* 1:1	*Point of Contact* **L.A. Bumm 405-364-7253, OU/Physics**	
File Name C:\Users\bmboo\Documents\Inventor\HeatEvaporator\heater\cable driven cart actuation\rail base.iam				

HOLE TABLE			
HOLE	XDIM	YDIM	DESCRIPTION
A1	.13	.25	8-32 UNC - 2B
A2	.63	.25	8-32 UNC - 2B

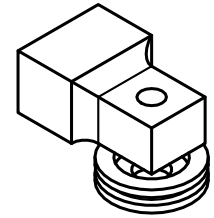

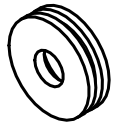

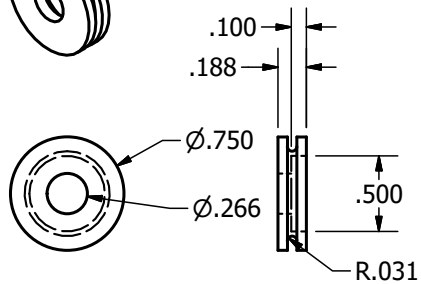

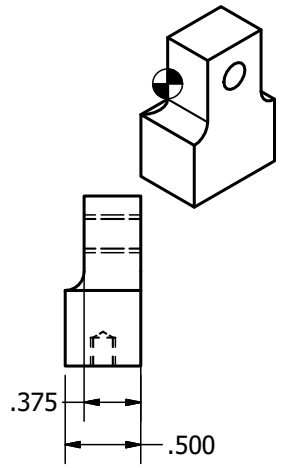

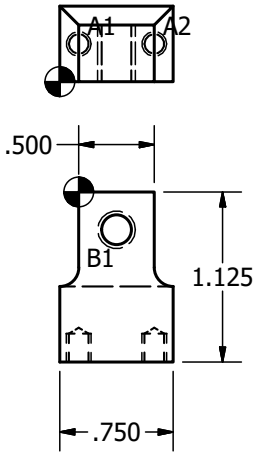

HOLE TABLE			
HOLE	XDIM	YDIM	DESCRIPTION
B1	.25	-.25	1/4-20 UNC - 2B

GALLOGLY COLLEGE OF ENGINEERING
SCHOOL OF AEROSPACE AND MECHANICAL ENGINEERING
The UNIVERSITY of OKLAHOMA

Drawn by Bryan Boone

Project Name	Material		Date	Revision	Sheet
Allara Thermal Evaporator, Lin Hall 120	Steel		7/28/2020	1	2 of 2
Part Name	**Quantity**	**Scale**	**Point of Contact**		
Rail Pulley	2	1:1	L.A. Bumm 405-364-7253, OU/Physics		
File Name C:\Users\bmboo\Documents\Inventor\HeatEvaporator\heater\cable driven cart actuation\rail base.iam					

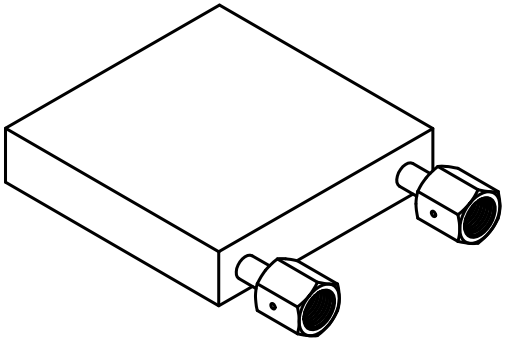

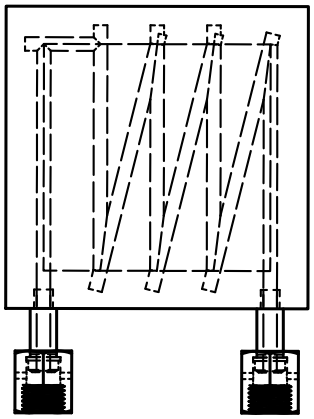

PARTS LIST			
ITEM	QTY	PART NUMBER	DESCRIPTION
1	1	copper plate with water lines	
2	2	pseudo VCR fitting butt long 9066N180_ULTRA-HIGH-POLISH BUTT-WELD FITTING	STEP AP203
3	2	pseudo VCR fitting female nut 9066N250_ULTRA-HIGH-POLISH BUTT-WELD FITTING	STEP AP203

GALLOGLY COLLEGE OF ENGINEERING
SCHOOL OF AEROSPACE AND MECHANICAL ENGINEERING
The UNIVERSITY of OKLAHOMA

Drawn by Bryan Boone

Project Name	Material		Date	Revision	Sheet
Allara Thermal Evaporator, Lin Hall 120	Copper		7/28/2020	1	1 of 2
Part Name	**Quantity**	**Scale**	**Point of Contact**		
Side Cooling Shields	2	1:2	L.A. Bumm 405-364-7253, OU/Physics		
File Name C:\Users\bmboo\Documents\Inventor\HeatEvaporator\heater\Side shutter Cooling Shield.iam					

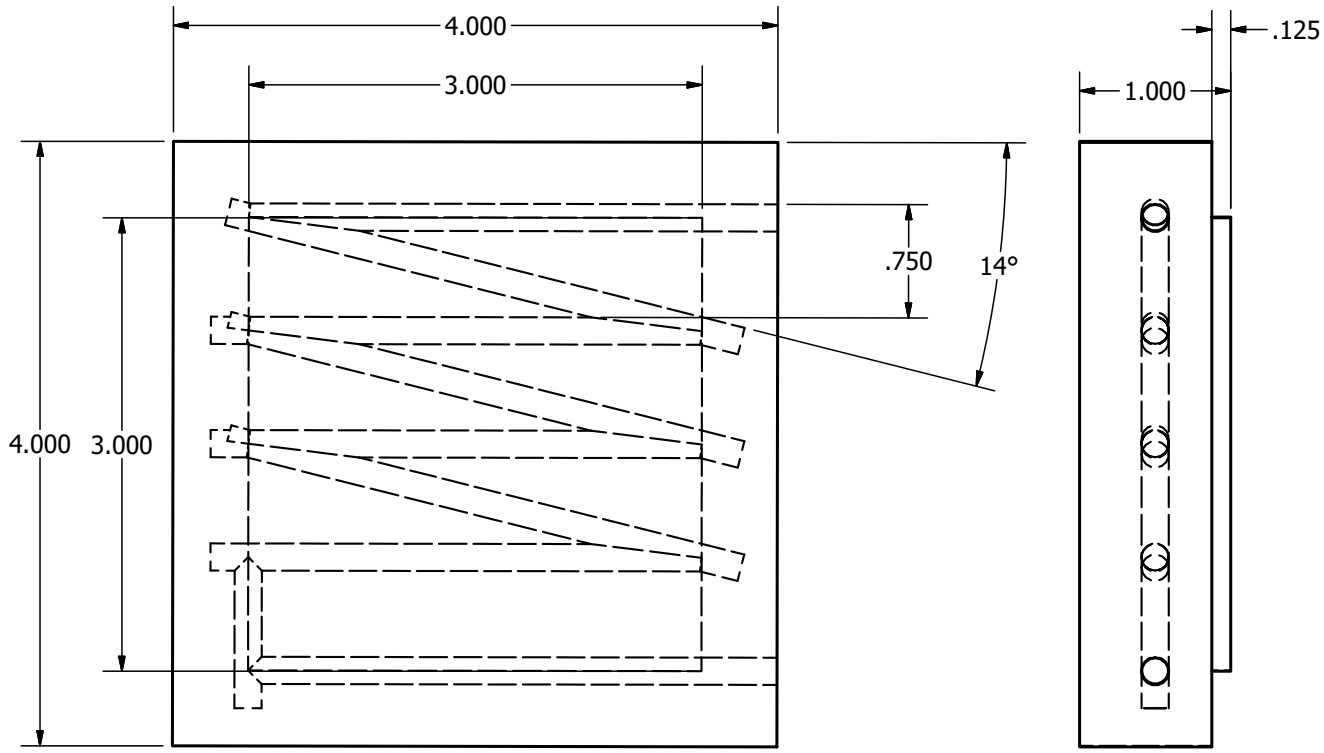

GALLOGLY COLLEGE OF ENGINEERING
SCHOOL OF AEROSPACE AND MECHANICAL ENGINEERING
The UNIVERSITY of OKLAHOMA

Drawn by Bryan Boone

Project Name	Material		Date	Revision	Sheet
Allara Thermal Evaporator, Lin Hall 120	Copper		7/28/2020	1	2 of 2
Part Name	**Quantity**	**Scale**	**Point of Contact**		
Side Shutter Cooler	2	1:1	L.A. Bumm 405-364-7253, OU/Physics		
File Name C:\Users\bmboo\Documents\Inventor\HeatEvaporator\heater\Side shutter Cooling Shield.iam					

Chapter 9

Appendices

PDFs of Spreadsheets and

ANSYS results appended

2989.0669 Pa/foot of water head 538.032042 kPa

0.4335 psi/foot of water head 0.000145038

6894.757293 **Q>=** 1.66667E-05 m^3/s

1 L/min

OD	ID	OD-A in^2	ID-A in^2	OD-A m^2	ID-A m^2	Q/A = **V** m/s (per correlating areas)		Lossless pressure, p Pa @20° C		25 °C (linear interpo)		30 °C	
0.125	0.07	0.012271846	0.003848451	7.9173E-06	2.48287E-06	2.105093591	6.712670889	2211.721	22489.42	2208.951599	22461.26	2206.182	22433.1
0.25	0.18	0.049087385	0.0254469	3.16692E-05	1.64173E-05	0.526273398	1.015187881	138.2326	514.3757	138.0594749	513.7315	137.8864	513.0874
0.375	0.31	0.110446617	0.075476764	7.12557E-05	4.86946E-05	0.233899288	0.342269379	27.3052	58.46873	27.2710074	58.39551	27.23681	58.3223
Possible VCR fitting sizes (mm. standards)													
OD	ID	OD-A mm^2	ID-A mm^2	OD-A m^2	ID-A m^2								
6	4	28.27433388	12.56637061	2.82743E-05	1.25664E-05	0.589462752	1.326291192	173.4204	877.941	173.2032819	876.8416	172.9861	875.7422
8	6	50.26548246	28.27433388	5.02655E-05	2.82743E-05	0.331572798	0.589462752	54.87131	173.4204	54.80260093	173.2033	54.73389	172.9861
10	8	78.53981634	50.26548246	7.85398E-05	5.02655E-05	0.212206591	0.331572798	22.47529	54.87131	22.44714534	54.8026	22.419	54.73389
12	10	113.0973355	78.53981634	0.000113097	7.85398E-05	0.147365688	0.212206591	10.83878	22.47529	10.82520512	22.44715	10.81163	22.419

Reynolds number, R (u is flow speed (m/s)) Re> 2900 (Above 2900 it's turbulent flow, below 2300 it's laminar, which's worse for heat transfer)

$$\mathrm{Re} = \frac{\rho u D_{\mathrm{H}}}{\mu}$$

	@Temp=	20 °C	25 °C (linear interpc	30 °C
	ρ, density, kg/m^3	998.2	996.95	995.7
	μ, dynamic viscosity, N*s/m^2	0.001002	0.0008985	0.000795

Haaland Eq. approximation of Darcy-weisbach friction factor

$$\frac{1}{\sqrt{f}} = -1.8\log\left[\left(\frac{\varepsilon/D}{3.7}\right)^{1.11} + \frac{6.9}{\mathrm{Re}}\right]$$

		D_H, m, hydraulic diameter	u m/s (minimum for turbulent flow) 20 °C	25 °C (linear interpo)	30 °C	Dynamic Pressure ~~p Pa (corresponding lossless pressure)~~ 20 °C	25 °C (linear interp	30 °C
	4	1.778	0.001778	1.637255271	1.469978372	1.302281475	1337.889867	1077.122932	844.3223
	6	3.175	0.003175	0.916862952	0.823187888	0.729277626	419.5622622	337.7857514	264.7795
	8	4	0.004	0.727759968	0.653405386	0.578864116	264.3406144	212.8182181	166.8214
	10	**4.572**	**0.004572**	**0.636710383**	**0.571658256**	**0.506442796**	**202.3351959**	**162.8982212**	**127.6907**
0.07	1.778	6	0.006	0.485173312	0.435603591	0.38590941	117.4847175	94.58587473	74.14285
0.125	3.175	6.35	0.00635	0.458431476	0.411593944	0.364638813	104.8905656	84.44643785	66.19486
0.25	6.35	7.874	0.007874	0.369702803	0.3319306	0.294063559	68.21706917	54.92094033	43.05077
0.375	9.525	8	0.008	0.363879984	0.326702693	0.289432058	66.08515359	53.20455454	41.70535
0.18	4.572	9.525	0.009525	0.305620984	0.274395963	0.243092542	46.61802914	37.53175016	29.41994
0.31	7.874	10	0.01	0.291103987	0.261362155	0.231545646	42.2944983	34.0509149	26.69142

ε/D (at higher Re, f goes higher, in an obtuse proportion)

D	@ ε= 0.001E-3 m	@ ε= 0.002E-3 m	f=	
0.001778	0.00056243	0.001125	0.0452	0.045609
0.003175	0.000314961	0.00063	0.04503	0.045247
0.004	0.00025	0.0005	0.044987	0.045156
0.004572	**0.000218723**	**0.000437**	**0.044967**	**0.045113**
0.006	0.000166667	0.000333	0.044934	0.045042
0.00635	0.00015748	0.000315	0.044929	0.04503
0.007874	0.000127	0.000254	0.04491	0.04499
0.008	0.000125	0.00025	0.044909	0.044987
0.009525	0.000104987	0.00021	0.044897	0.044962
0.01	0.0001	0.0002	0.044894	0.044955

Without Dynamic pressure number

1 meter and pressure drop at velocity for ε=0.002E-3

P_sum kPa, Sum of major losses

D, m	20 °C	25 °C (linear interpo)	30 °C
0.001778	34.31973	27.6305014	21.65866734
0.003175	5.979229	4.813822967	3.773402037
0.004	2.984135	2.402500209	1.883243161
0.004572	**1.996476**	**1.607344751**	**1.2599462**
0.006	0.881962	0.710059628	0.556593059
0.00635	0.743814	0.598838211	0.469410143
0.007874	0.389775	0.313803923	0.24598087
0.008	0.371625	0.299191743	0.234526849
0.009525	0.220055	0.177164403	0.138873516
0.01	0.190136	0.153077126	0.119992269
	psi		
0.001778	4.977656	4.007465415	3.141324113
0.003175	0.867214	0.698185993	0.547285695
0.004	0.432812	0.348453195	0.273141328
0.004572	**0.289564**	**0.233125646**	**0.182739747**
0.006	0.127918	0.102985442	0.080726998
0.00635	0.107881	0.086854139	0.068082185
0.007874	0.056532	0.045513411	0.035676509
0.008	0.0539	0.043394093	0.034015244
0.009525	0.031916	0.025695524	0.020141901
0.01	0.027577	0.02220196	0.017403407

1 meter and pressure drop at velocity for ε=0.002E-3

P_sum kPa, Sum of major losses '@

D, m	20 °C	25 °C (linear interp	30 °C
0.001778	35.65761953	28.70762433	2.050299
0.003175	6.398791539	5.151608718	4.038181
0.004	2.248476027	2.615318471	2.050065
0.004572	**2.098811355**	**1.770247572**	**1.387637**
0.006	0.995246798	0.804655503	0.630736
0.00635	0.848[illegible]991	0.68[illegible]284649	0.535605
0.007874	0.457991[illegible]3	0.368724863	0.289032
0.008	0.4377095	0.352396297	0.276232
0.009525	0.26667319	0.214696153	0.168293
0.01	0.232430954	0.187128041	0.146684
	psi		
0.001778	5.171[illegible]047	4.1[illegible]3688888	3.263783
0.003175	0.928[illegible]6249	0.74[illegible]77674	0.585689
0.004	0.4[illegible]151614	0.379[illegible]868	0.297337
0.004572	**0.[illegible]18910625**	**0.256752[illegible]6**	**0.20126**
0.006	0.144957503	0.11670396[illegible]	0.091481
0.00635	0.123094252	0.09910206	0.077683
0.007874	0.066426066	0.05347902	0.04192
0.008	0.063484462	0.051110762	0.04[illegible]064
0.009525	0.038677676	0.031139044	0.024[illegible]
0.01	0.03371126	0.027140628	0.0212[illegible]

Darcy Weischbach eq. for pressure lost to friction, known as major losses

$$\frac{\Delta p}{L} = f_{\mathrm{D}} \cdot \frac{\rho}{2} \cdot \frac{\langle v \rangle^2}{D},$$

Δp/L, Pa/m

D, m	@ ε= 0.001E-3 m 20 °C	25 °C (line	30 °C	@ ε= 0.002E-3 m 20 °C	25 °C (line	30 °C
0.001778	34011.27012	27382.16	21464.00314	34319.73	27630.5	21658.67
0.003175	5950.515402	4790.706	3755.281141	5979.229	4813.823	3773.402
0.004	2972.998448	2393.534	1876.21479	2984.135	2402.5	1883.243
0.004572	**1990.039528**	**1602.163**	**1255.884139**	**1996.476**	**1607.345**	**1259.946**
0.006	879.8522467	708.361	555.2615742	881.9621	710.0596	556.5931
0.00635	742.1426386	597.4923	468.3551032	743.8144	598.8382	469.4101
0.007874	389.0832649	313.2474	245.5446206	389.7745	313.8039	245.9809
0.008	370.9771595	298.6703	234.1181288	371.6248	299.1917	234.5268
0.009525	219.7388026	176.9097	138.673867	220.0552	177.1644	138.8735
0.01	189.8774066	152.8686	119.8287873	190.1365	153.0771	119.9923

Summary

Project:	**roughDraftHeating2**
Date:	**7/30/2020**
Time:	**10:08:02 AM**
Product Version:	**2019 R3**
Last Saved Version:	**2019 R3**

Project Schematic Pane

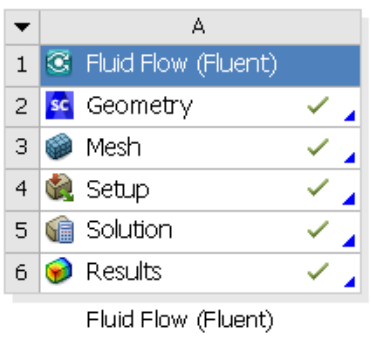

Files

Name	Size	Type	Date Modified	Location
FFF.scdoc	1 MB	Geometry File	4/7/2020 1:48:43 AM	dp0\FFF\DM
FFF.mshdb	12 MB	Mesh Database File	4/7/2020 2:54:03 AM	dp0\global\MECH
roughDraftHeating2.wbpj	45 KB	Workbench Project File	6/9/2020 8:45:46 AM	C:\Users\bmboo\Documents\Inventor\HeatEvaporator\heater
FFF.set	305 KB	FLUENT Model File	4/7/2020 3:25:26 AM	dp0\FFF\Fluent
FFF.msh	16 MB	Fluent Mesh File	4/7/2020 2:43:44 AM	dp0\FFF\MECH
FFF-Setup-Output.cas.gz	15 MB	FLUENT Case File	4/7/2020 2:50:04 AM	dp0\FFF\Fluent
FFF.ip	33	FLUENT	4/7/2020	dp0\FFF\Fluent

	MB	Interpolation Data File	3:29:11 AM	
FFF-1.cas.gz	17 MB	FLUENT Case File	4/7/2020 3:30:21 AM	dp0\FFF\Fluent
FFF-1-00142.dat.gz	24 MB	FLUENT Data File	4/7/2020 3:30:27 AM	dp0\FFF\Fluent
Fluid Flow Fluent.cst	38 KB	CFD-Post State File	6/2/2020 3:14:41 AM	dp0\FFF\Post
fluent-0-error.log	165 B	.log	4/7/2020 2:28:17 AM	dp0\FFF\MECH
fluent-1-error.log	110 B	.log	4/7/2020 2:28:17 AM	dp0\FFF\MECH
fluent-2-error.log	110 B	.log	4/7/2020 2:28:17 AM	dp0\FFF\MECH
fluent-3-error.log	110 B	.log	4/7/2020 2:28:17 AM	dp0\FFF\MECH
fluent-4-error.log	110 B	.log	4/7/2020 2:28:17 AM	dp0\FFF\MECH
fluent-5-error.log	110 B	.log	4/7/2020 2:28:17 AM	dp0\FFF\MECH
fluent-6-error.log	110 B	.log	4/7/2020 2:28:17 AM	dp0\FFF\MECH
fluent-7-error.log	110 B	.log	4/7/2020 2:28:17 AM	dp0\FFF\MECH
fluent-999999-error.log	180 B	.log	4/7/2020 2:28:17 AM	dp0\FFF\MECH
MPT_Monitor_system.0.dbg	130 B	.dbg	4/7/2020 2:28:17 AM	dp0\FFF\MECH
MPT_Monitor_system.999999.dbg	616 B	.dbg	4/7/2020 2:28:17 AM	dp0\FFF\MECH
designPoint.wbdp	43 KB	Workbench Design Point File	6/9/2020 8:45:46 AM	dp0
report.xml	10 KB	.xml	4/7/2020 3:25:29 AM	progress_files\dp0\FFF\Fluent
Solution.trn	1 KB	.trn	4/7/2020 2:13:32 AM	progress_files\dp0\FFF\Fluent
AnsysReportLogo.png	6 KB	.png	7/28/2019 1:02:44 PM	user_files\roughDraftHeating2_report_images
ProjectSchematic.png	8 KB	.png	7/30/2020 10:08:02 AM	user_files\roughDraftHeating2_report_images

FFF : Solution : dp0

```
Fluent
Version: 3d, dp, pbns, ske (3d, double precision, pressure-based, standard k-epsilon)
Release: 19.5.0
Title:


Models
------

   Model                        Settings
   ---------------------------------------------------------------
   Space                        3D
   Time                         Steady
   Viscous                      Standard k-epsilon turbulence model
   Wall Treatment               Standard Wall Functions
   Heat Transfer                Enabled
   Solidification and Melting   Disabled
   Radiation                    None
   Species                      Disabled
   Coupled Dispersed Phase      Disabled
   NOx Pollutants               Disabled
   SOx Pollutants               Disabled
   Soot                         Disabled
   Mercury Pollutants           Disabled
   Structure                    Disabled


Material Properties
-------------------

   Material: water-liquid (fluid)

      Property                        Units     Method     Value(s)
      ---------------------------------------------------------------
      Density                         kg/m3     constant   998.2
      Cp (Specific Heat)              j/kg-k    constant   4182
      Thermal Conductivity            w/m-k     constant   0.6
      Viscosity                       kg/m-s    constant   0.001003
      Molecular Weight                kg/kmol   constant   18.0152
      Thermal Expansion Coefficient   1/k       constant   0
      Speed of Sound                  m/s       none       #f

   Material: fluid-1 (fluid)

      Property                        Units     Method     Value(s)
      ----------------------------------------------------------------
      Density                         kg/m3     constant   1.225
      Cp (Specific Heat)              j/kg-k    constant   1006.43
      Thermal Conductivity            w/m-k     constant   0.0242
      Viscosity                       kg/m-s    constant   1.7894e-05
      Molecular Weight                kg/kmol   constant   28.966
      Thermal Expansion Coefficient   1/k       constant   0
      Speed of Sound                  m/s       none       #f

   Material: copper (solid)

      Property               Units    Method     Value(s)
      ---------------------------------------------------
      Density                kg/m3    constant   8978
      Cp (Specific Heat)     j/kg-k   constant   381
      Thermal Conductivity   w/m-k    constant   387.6

   Material: solid-1 (solid)

      Property               Units    Method     Value(s)
      ---------------------------------------------------
      Density                kg/m3    constant   2719
      Cp (Specific Heat)     j/kg-k   constant   871
      Thermal Conductivity   w/m-k    constant   202.4
```

```
   Material: air (fluid)

      Property                        Units     Method     Value(s)
      ------------------------------------------------------------
      Density                         kg/m3     constant   1.225
      Cp (Specific Heat)              j/kg-k    constant   1006.43
      Thermal Conductivity            w/m-k     constant   0.0242
      Viscosity                       kg/m-s    constant   1.7894e-05
      Molecular Weight                kg/kmol   constant   28.966
      Thermal Expansion Coefficient   1/k       constant   0
      Speed of Sound                  m/s       none       #f

   Material: aluminum (solid)

      Property               Units    Method     Value(s)
      ---------------------------------------------------
      Density                kg/m3    constant   2719
      Cp (Specific Heat)     j/kg-k   constant   871
      Thermal Conductivity   w/m-k    constant   202.4


Cell Zone Conditions
--------------------

   Zones

      name              id   type
      ----------------------------
      walls_2_walls_1   5    solid
      volume_pipes      4    fluid

   Setup Conditions

      walls_2_walls_1

         Condition       Value
         ---------------------
         Frame Motion?   no

      volume_pipes

         Condition       Value
         ---------------------
         Frame Motion?   no


Boundary Conditions
-------------------

   Zones

      name                                                  id   type
      ---------------------------------------------------------------------------
      contact_region-wall1-1-1-shadow                       24   wall
      contact_region-wall1-1-1                              21   wall
      contact_region-trg-non-overlapping                    23   wall
      conductance_walls-contact_region-src-non-overlapping  22   wall
      wall-walls_2_walls_1                                  1    wall
      inlet                                                 8    velocity-inlet
      outlet                                                9    pressure-outlet
      conductance_walls                                     10   wall
      radiative_walls                                       11   wall
      conductance_walls-contact_region-src                  12   interface
      contact_region-trg                                    13   interface

   Setup Conditions

      contact_region-wall1-1-1-shadow

         Condition         Value
```

```
   -----------------------
   Thermal BC Type   3

contact_region-wall1-1-1

   Condition                  Value
   -------------------------------
   Thermal BC Type            3
   Wall Motion                0
   Shear Boundary Condition   0

contact_region-trg-non-overlapping

   Condition         Value
   -----------------------
   Thermal BC Type   1

conductance_walls-contact_region-src-non-overlapping

   Condition                  Value
   -------------------------------
   Thermal BC Type            1
   Wall Motion                0
   Shear Boundary Condition   0

wall-walls_2_walls_1

   Condition         Value
   --------------------------
   Material Name     aluminum
   Thermal BC Type   1

inlet

   Condition                  Value
   -------------------------------
   Velocity Magnitude (m/s)   1

outlet

   Condition   Value
   -----------------

conductance_walls

   Condition                  Value
   ----------------------------------
   Material Name              aluminum
   Thermal BC Type            1
   Wall Motion                0
   Shear Boundary Condition   0

radiative_walls

   Condition          Value
   ------------------------
   Thermal BC Type    1
   Heat Flux (w/m2)   26000

conductance_walls-contact_region-src

   Condition   Value
   -----------------

contact_region-trg

   Condition   Value
   -----------------
```

```
Solver Settings
---------------

   Equations

      Equation     Solved
      -------------------
      Flow         yes
      Turbulence   yes
      Energy       yes

   Numerics

      Numeric                          Enabled
      ---------------------------------------
      Absolute Velocity Formulation   yes

   Relaxation

      Variable                     Relaxation Factor
      ----------------------------------------------
      Density                      1
      Body Forces                  1
      Turbulent Kinetic Energy     0.75
      Turbulent Dissipation Rate   0.75
      Turbulent Viscosity          1
      Energy                       0.75

   Linear Solver

                                   Solver    Termination   Residual Reduction
      Variable                     Type      Criterion     Tolerance
      ---------------------------------------------------------------------
      Flow                         F-Cycle   0.1
      Turbulent Kinetic Energy     F-Cycle   0.1
      Turbulent Dissipation Rate   F-Cycle   0.1
      Energy                       F-Cycle   0.1

   Pressure-Velocity Coupling

      Parameter                             Value
      -------------------------------------------
      Type                                  Coupled
      Pseudo Transient                      yes
      Explicit momentum under-relaxation    0.5
      Explicit pressure under-relaxation    0.5

   Discretization Scheme

      Variable                     Scheme
      ---------------------------------------------
      Pressure                     Second Order
      Momentum                     Second Order Upwind
      Turbulent Kinetic Energy     First Order Upwind
      Turbulent Dissipation Rate   First Order Upwind
      Energy                       Second Order Upwind

   Solution Limits

      Quantity                          Limit
      ---------------------------------------
      Minimum Absolute Pressure         1
      Maximum Absolute Pressure         5e+10
      Minimum Temperature               1
      Maximum Temperature               5000
      Minimum Turb. Kinetic Energy      1e-14
      Minimum Turb. Dissipation Rate    1e-20
      Maximum Turb. Viscosity Ratio     100000
```

qty	thread	length	vented/unvented	assembly	nut or bolt	
8	8-32	0.750	unvented	top heater	bolt	
2	1/4-20		spring top plate	spring top plate	nut	
2	1/4-20	0.750	spring top plate	spring top plate	bolt	
4	8-32		unvented	spring top plate	nut	
2	8-32	0.750	unvented	spring top plate	bolt	
1	8-32	1.000	vented	lifting subassembly	bolt	
1	8-32		unvented	lifting subassembly	thin nut	
6	8-32	6.000	unvented	lifting subassembly	bolt	
8	6-32	0.375	unvented	heater holder assembl	bolt	
2	1/4-20	1.500	unvented	Extraneous Support	bolt	
2	1/4-20		unvented	Extraneous Support	nut	
8	8-32	1.000	unvented	Extraneous Support	bolt	
4	1/4-20	0.500	unvented	nuBottomCart	bolt	
2	8-32	0.500	unvented	nuBottomCart	bolt	
1	8-32	1.500	unvented	assembled v2 cord cap	bolt	
1	8-32		unvented	assembled v2 cord cap	nut	
2	8-32	0.500	vented	assembled v2 cord cap	bolt	
12			unvented	throughout	conical spring washers	
4	8-32	0.250	vented	rail mount for pulleys	bolt	needs to be flat head
3	8-32	2.000	unvented	spool redux	bolt	
7	8-32		unvented	spool redux	nut	
1	8-32	0.750	unvented	spool redux	bolt	
2	8-32	0.500	unvented	spool redux	bolt	retaining bolt for rod mount base
8	8-32	0.500	unvented	top heater	helicoil inserts	

References

[1] *1960 - Metal Oxide Semiconductor (MOS) Transistor Demonstrated*. URL: https://www.computerhistory.org/siliconengine/metal-oxide-semiconductor-mos-transistor-demonstrated/ (visited on 06/20/2020).

[2] *Accessories - Rotary & Linear Motion Radial Ball Bearing - MDC Vacuum Products, LLC*. [Online; accessed 10. Jul. 2020]. July 2020. URL: https://www.mdcvacuum.com/Products/US/Product/Radial-Ball-Bearing/Section/m727/Category/m.7.2/Radial_Ball_Bearing.

[3] Jack P. Holman. *Heat Transfer*. 10th ed. McGraw-Hill Education, Jan. 2009, pp. 416–419. ISBN: 978-007352936-3. URL: https://books.google.com/books/about/Heat_Transfer.html?id=7TGGPwAACAAJ.

[4] Y. Kuo. "Thin Film Transistor Technology–Past, Present, and Future". In: *Interface magazine* 22.1 (Jan. 2013), pp. 55–61. DOI: 10.1149/2.f06131if. URL: https://doi.org/10.1149%2F2.f06131if.

[5] *Kurt J. Lesker Company*. [Online; accessed 27. Jun. 2020]. June 2020. URL: https://www.lesker.com/newweb/deposition_materials/materialdepositionchart.cfm?pgid=0.

[6] *MTI Corp - Leading provider of lab equipments and advanced crystal substrates*. [Online; accessed 6. Jul. 2020]. July 2020. URL: https://www.mtixtl.com/epithinfilmonsubstrate.aspx.

[7] T. L. Perelman. "On conjugated problems of heat transfer". In: *Int. J. Heat Mass Transfer* 3.4 (Dec. 1961), pp. 293–303. ISSN: 0017-9310. DOI: 10.1016/0017-9310(61)90044-8.

[8] Michael J. Pratt. "Introduction to ISO 10303—the STEP Standard for Product Data Exchange". In: *J. Comput. Inf. Sci. Eng.* 1.1 (Mar. 2001), pp. 102–103. ISSN: 1530-9827. DOI: 10.1115/1.1354995.

[9] *Table of Emissivity of Various Surfaces*. [Online; accessed 17. Jul. 2020]. Mikron Instrument Company, Inc. Aug. 2003. URL: http://www-eng.lbl.gov/~dw/projects/DW4229_LHC_detector_analysis/calculations/emissivity2.pdf.

[10] *THIN FILMS - LEBOW*. [Online; accessed 6. Jul. 2020]. July 2020. URL: https://lebowcompany.com/thin-films.

[11] Vacuum Technique, part of the Atlas Copco Group. *The Fundamentals of Vacuum Science - Vacuum Science World*. [Online; accessed 17. Jul. 2020]. July 2020. URL: https://www.vacuumscienceworld.com/vacuum-science#vacuum_physics_-_basic_terms.

[12] Robert K. Waits. "Edison's vacuum coating patents". In: *Journal of Vacuum Science & Technology A* 19.4 (2001), pp. 1666–1673. DOI: 10.1116/1.1326948. eprint: https://doi.org/10.1116/1.1326948. URL: https://doi.org/10.1116/1.1326948.